Tonkin+Taylor

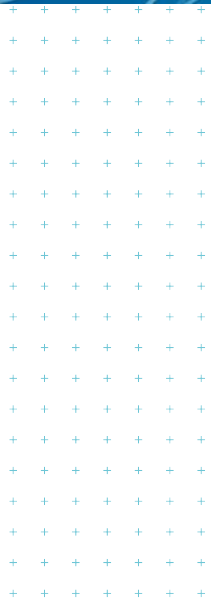# Glenorchy Liquefaction Vulnerability Assessment

Prepared for
Otago Regional Council
Prepared by
Tonkin & Taylor Ltd
Date
May 2022
Job Number
1017916

Exceptional thinking together
www.tonkintaylor.co.nz

Document Control

Title:	Glenorchy Liquefaction Vulnerability Assessment				
Date	**Version**	**Description**	**Prepared by:**	**Reviewed by:**	**Authorised by:**
28/01/2022	0.1	Draft for Peer Review and Consultation	NAMC	ERBI	SVB
12/05/2022	0.2	Revised draft responding to peer review comments for Peer Review and Consultation	NAMC	ABL, SVB	SVB
26/05/2022	1	Report for Issue to ORC	NAMC	SVB	SVB

Distribution:

Otago Regional Council   1 PDF copy

Tonkin & Taylor Ltd (FILE)   1 PDF copy

4

Table of contents

Tonkin & Taylor Ltd   May 2022
Glenorchy Liquefaction Vulnerability Assessment   Job No: 1017916
Otago Regional Council

LIQUEFACTION ASSESSMENT SUMMARY	
This liquefaction assessment has been undertaken in general accordance with the guidance document 'Assessment of Liquefaction-induced Ground Damage to Inform Planning Processes' published by the Ministry of Business, Innovation and Employment and the Ministry for the Environment in 2017 (MBIE & MfE, 2017). https://www.building.govt.nz/building-code-compliance/b-stability/b1-structure/planning-engineering-liquefaction-land/	
Client	Otago Regional Council (ORC)
Assessment undertaken by	Tonkin & Taylor Ltd, PO Box 13-055, Christchurch 8141
Extent of the study area	The Glenorchy Township, as shown in Figure 2.1 in Section 2.
Intended RMA planning and consenting purposes	To provide ORC with a liquefaction vulnerability assessment to help inform spatial planning and assessment of land use, subdivision and building consents in Glenorchy.
Other intended purposes	To provide ORC with an understanding of expected land performance for a range of potential future earthquake scenarios.
Level of detail	Level C (detailed area-wide assessment).
Notes regarding base information	The assessment leverages previous work conducted over the study area which includes: • Geotechnical investigation data available on the NZ Geotechnical Database (MBIE, 2022), • A LiDAR DEM provided by ORC, along with Bathymetry data from NIWA via ORC, and • Groundwater level monitoring undertaken by e3 Scientific (e3 Scientific Ltd., 2018)
Other notes	This assessment is intended to approximately describe the typical range of liquefaction vulnerability across Glenorchy. It is not intended to serve as a site-specific assessment, nor to precisely describe liquefaction vulnerability at an individual-property scale. This information is general in nature, and more detailed site-specific liquefaction assessment may be required for some purposes (e.g., for design of building foundations).

1 Scope of Work

Otago Regional Council (ORC) have engaged Tonkin + Taylor (T+T) to carry out an assessment of liquefaction hazard in Glenorchy township. ORC's objectives are to quantify the liquefaction and lateral spreading hazard for a range of seismic scenarios to assist ORC in making risk management and adaptation decisions.

The assessment undertaken in this study has been in accordance with the Ministry of Business, Innovation and Employment (MBIE) & Ministry for the Environment (MfE) guidance document: *Planning and engineering guidance for potentially liquefaction prone land*, (MBIE & MfE, 2017), henceforth referred to as "the MBIE/MfE Guidance". Following this document, the present study entails a risk-based assessment of liquefaction vulnerability across the township.

The spatial extent of the study includes the township area bounded by the Glenorchy lagoon, the Lake Wakatipu foreshore, the Buckler Burn, and the base of Bible Terrace (shown in Figure 2.1, below).

This study is solely an assessment of the liquefaction hazard at Glenorchy. There are various other natural hazards and geotechnical constraints which would also need to be considered as part of any future land development or building activities. It is emphasized that discussion in this report, especially references to "vulnerability categories" relates only to liquefaction hazard and not any other natural hazards.

2 Site Description

Glenorchy township is located at the head of Lake Wakatipu, approximately 30 km northwest of Queenstown and 40 km southeast of Milford Sound. The site location is shown in Figure 2.1 below.

Figure 2.1: Glenorchy township location. The approximate location of the Alpine Fault is shown in red. The study area for this project is shown outlined in blue on the inset map.

3 Liquefaction Hazard in General

Liquefaction is a natural process where earthquake shaking increases the water pressure in the ground in some types of soil, resulting in temporary loss of soil strength.

The following three key elements are all required for liquefaction to occur:

- Sufficient ground shaking (a combination of the duration and intensity of shaking);
- A loose-to-medium-dense granular soil material (typically sands and silts, or in some cases gravel); and
- That these soils are saturated (i.e., below the groundwater table).

The severity of the liquefaction hazard therefore depends on the strength and duration of the earthquake shaking, the thickness and density of the granular soils and the depth of the groundwater table.

Figure 3.1 provides a schematic representation of the liquefaction process. For a more detailed explanation, refer to the MBIE/MfE Guidance (MBIE & MfE, 2017) from which these diagrams are reproduced.

The liquefaction process

Soil particles Pore water Ground surface subsidence

Before earthquake During earthquake After earthquake

Formation of liquefaction ejecta

Ground surface Water and sand Ground surface subsidence Sand boil

Non-liquefying crust

Loose to medium dense liquefying sand layer

Densified sand

Densified sand

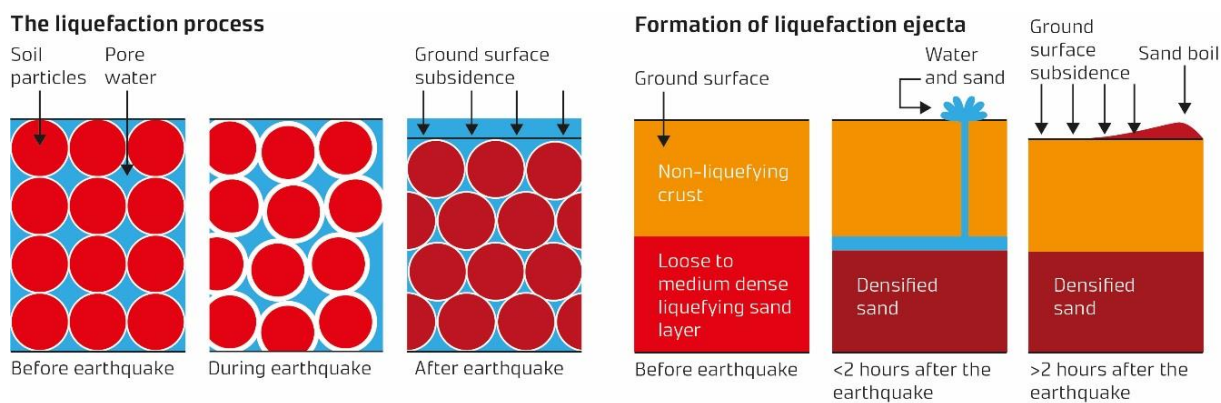Before earthquake <2 hours after the earthquake >2 hours after the earthquake

Figure 3.1: Schematic representation of the process of liquefaction and the manifestation of liquefaction ejecta. Reproduced from the MBIE/MfE Guidance (2017).

Liquefaction can give rise to significant land and building damage through multiple mechanisms, giving rise both to vertical settlement and sometimes also lateral/horizontal movement (*lateral spreading*), typically towards a lake, river, or other depressed water body, including large cracking in the ground. Some of these effects are illustrated in Figure 3.2. Appendix B provides a selection of maps and photos showing examples of the liquefaction and lateral spreading that was observed following the 2010-2011 Canterbury earthquakes and 2016 Kaikoura earthquakes.

Vertical settlement is often highly variable rather than uniform. Figure B1 in Appendix B provides a map showing the ground surface settlement that occurred due to liquefaction in the 2010 – 2011 Canterbury earthquakes. It is caused by several compounding factors, including:

- *Volumetric consolidation*: where the earthquake shaking causes the loose sand particles to pack more tightly together resulting in settlement of the ground surface (see Figure 3.1);
- *Liquefaction ejecta*: where large quantities of water and sediment come out of the ground and are deposited at the ground surface resulting in additional settlement. Refer to Figures B10, B11 and B12 in Appendix B for examples; and
- Vertical drops caused by lateral spreading. Refer to Figures B3, B5 and B9 in Appendix B for examples.

Lateral spreading is a type of liquefaction-induced ground failure that occurs in areas with gentle slopes or with a free face in close proximity such as a river bank, lake edge or other depressed water body. Figure B2 in Appendix B provides a map showing the lateral spreading that occurred due to liquefaction in the 2010 – 2011 Canterbury earthquakes. Lateral spreading can result in significant total and differential, horizontal and vertical ground movement causing ground tearing and cracking, with areas close to the free face having the highest risk of lateral spread induced damage. Lateral spreading is often the cause of the most severely affected ground in liquefaction damaged areas, and therefore often results in the most significant damage to buildings and other infrastructure (refer to Figures B3 to B9 in Appendix B for examples).

In Glenorchy, there is a free face of up to 25m on the lakebed, roughly 30m away from the shore. For comparison: following the Canterbury Earthquake Sequence, the areas that were most severely affected by lateral spreading in the residential red zone areas of Christchurch adjacent to the Avon River had free face heights of about 4m. This means that the lateral spreading in Glenorchy is likely to be considerably worse compared to the lateral spreading that occurred in Christchurch following the 2010 – 2011 Canterbury earthquakes. Sections 7 and 13 explain this in further detail.
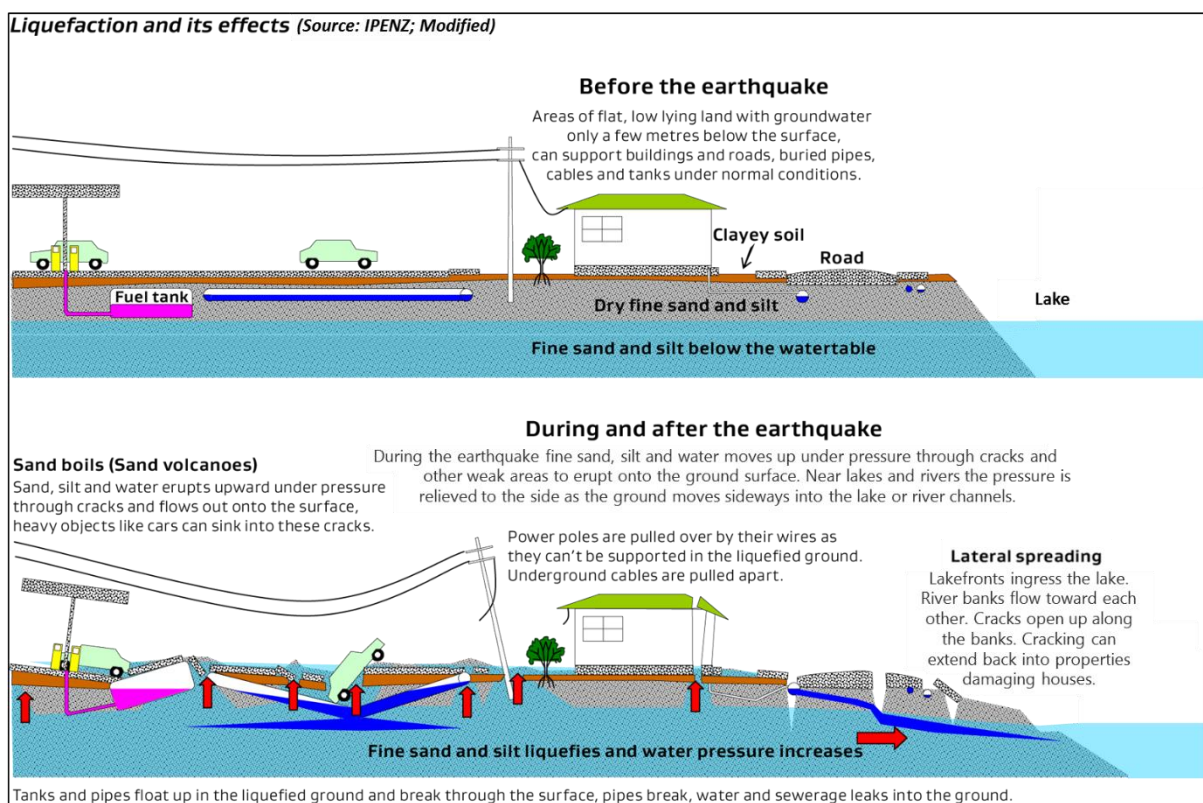

Figure 3.2: Visual schematic of the consequences of liquefaction. Reproduced from the MBIE/MfE Guidance (2017) with modification for the context of a lake.

4 The MBIE/MfE Guidance

The MBIE/MfE Guidance (MBIE & MfE, 2017) presents a risk-based approach for the management of liquefaction-related risk in land use planning and development decision-making. The guidance was developed in response to the Canterbury Earthquake Sequence 2010–2011 following recommendations made by the Royal Commission of Inquiry into Building Failure caused by the Canterbury Earthquakes.

For the purposes of categorizing the liquefaction vulnerability of land, the MBIE/MfE Guidance specifies a performance-based framework to inform planning and consenting processes. That framework is based on the severity of liquefaction-induced ground damage that is expected to occur at various intensities of earthquake shaking. Figure 4.1 shows the recommended liquefaction vulnerability categories for use in that performance-based framework.
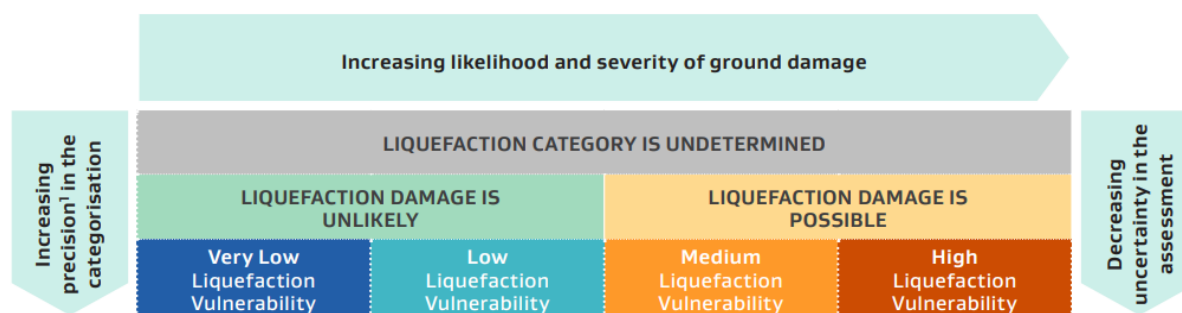
Note:

1   In this context the 'precision' of the categorisation means how explicitly the level of liquefaction vulnerability is described. The precision is different to the accuracy (ie trueness) of the categorisation.

Figure 4.1: Recommended liquefaction vulnerability categories for use in liquefaction assessment studies to inform planning and consenting processes. Reproduced from the MBIE/MfE Guidance (2017).

As shown in Figure 4.1, the liquefaction vulnerability categories established in the MBIE/MfE have varying levels of precision in the categorisation based on the degree of uncertainty in the assessment. Highly precise categorizations are not justified if there are high levels of uncertainty in the assessment. The uncertainty depends on a number of factors including an understanding of the seismicity, geological factors, subsurface variability, groundwater, the availability of subsurface geotechnical test data, among other things.

Less precise categorizations may not be sufficient for some applications, so the MBIE/MfE Guidance provides recommendations for the minimum level of detail required in the liquefaction assessment for a variety of specific applications. Figure 4.2 shows the categories used to define the levels of detail for liquefaction vulnerability studies.

The present study has been carried out at a Level C level of detail – a detailed area-wide assessment.

Figure 4.2: Categories of level of detail used to define the levels of detail for liquefaction vulnerability studies. Reproduced from the MBIE/MfE Guidance (2017).

5   Seismicity

For a Level C level of detail, the MBIE/MfE Guidance recommends considering multiple different earthquake scenarios when assessing liquefaction vulnerability. Larger earthquakes have the potential to cause more severe liquefaction damage than smaller ones, but smaller earthquakes can occur more frequently. Determining representative seismic scenarios for the study requires an understanding of the seismotectonic context around the Glenorchy township study area.

Glenorchy is positioned on the Pacific tectonic plate, east of the Australian-Pacific tectonic plate boundary (that is, the Alpine Fault). The relative displacement between the Australian and Pacific tectonic plates is largely taken up along a single dextral (right lateral) strike-slip movement along the Alpine Fault. The remainder of the plate motion is taken up by and expressed on numerous smaller active faults. Known active faults in the lower South Island included in the development of the 2012 New Zealand Seismic Hazard model's fault source model are illustrated in Figure 5.1, which has been reproduced from a report on that Model (Stirling, et al., 2012).
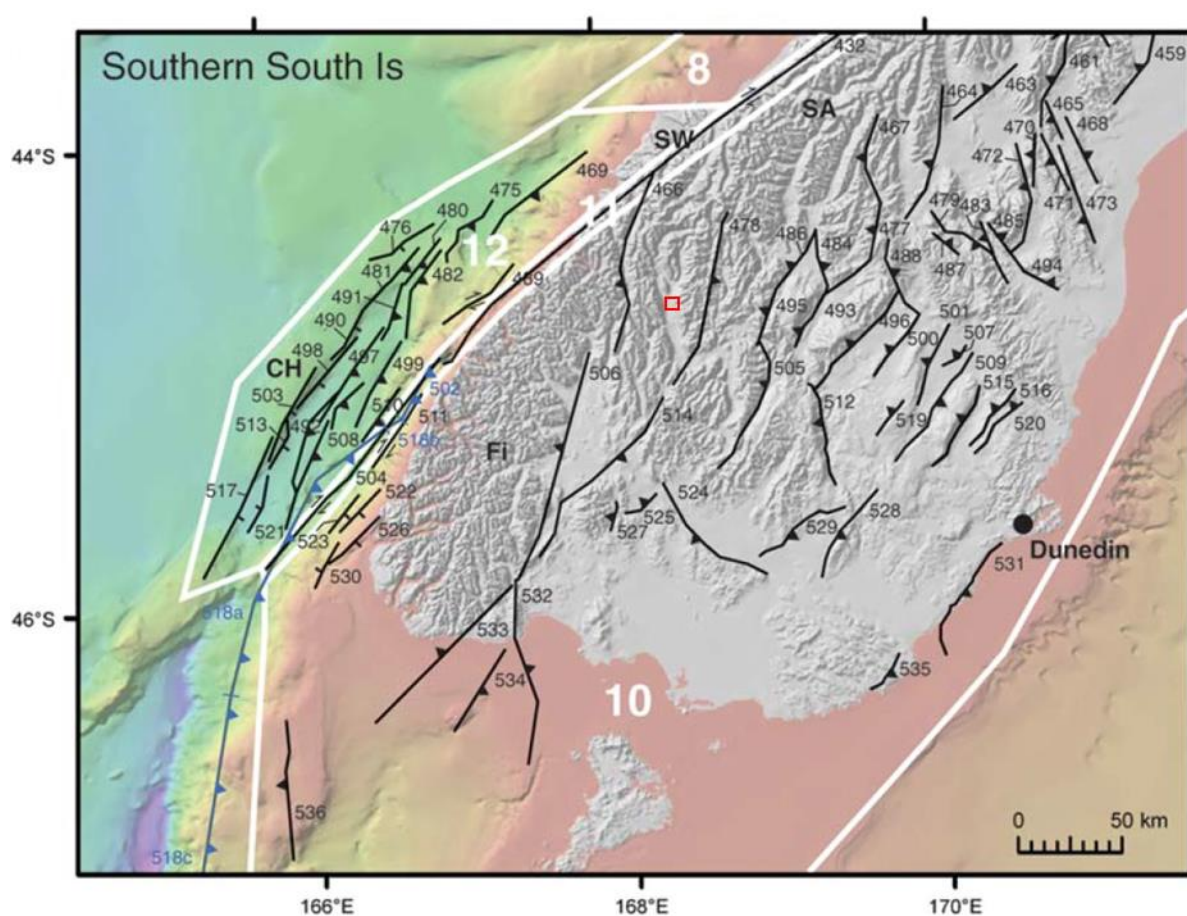

Figure 5.1: Known active faults in the Southern South Island, shown by the black lines with directional arrows (with annotated ID numbers ranging from 432 up to 536). Glenorchy is outlined with a red box. Reproduced from Figure 3(e) the National Seismic Hazard Model (NSHM) for New Zealand (Stirling, et al., 2012).

There are numerous earthquake faults in the region that can produce strong shaking which would affect the Glenorchy township. The main ones are the Alpine Fault (annotated as area 11 in Figure 5.1), the Hollyford Fault (the southern segment of the line annotated as 466), and the Greenstone Fault; all of which are located to the west of Glenorchy; also, the West Wakatipu fault located to the south; and the Moonlight Fault (annotated as 478) located to the east of Glenorchy. Of these faults, the Alpine Fault is the furthest away, but is also the most active (in the sense that it has the most

frequent recurrence intervals). Glenorchy is located approximately 55 km from the nearest point on the Alpine Fault (shortest horizontal distance).

For this study, a range of different earthquake scenarios have been considered, ranging from a smaller 25-year event up to a larger 2500-year event, incorporating an allowance for uncertainty in the seismic hazard running lower bound and upper bound ground motions. In addition, an Alpine Fault Rupture Scenario has been considered (with a return period of approximately 30-years) for 16%, 50% and 84% ground motion levels.

As recommended in Module 1 of the Guidelines for earthquake geotechnical engineering practice in New Zealand (NZGS & MBIE, 2021a), the return periods for our scenarios have been determined using Table A1 from Appendix A of the 2021 guidelines to determine the earthquake magnitude (M_w) and the earthquake shaking intensity (which is measured as a Peak Ground Acceleration (PGA) and expressed as a proportion of the acceleration due to gravity, g). Note that Glenorchy is not listed in Table A1 from Appendix A of the 2021 guidelines, so interpolation was necessary to determine the M_w and PGA for the various return periods as discussed below.

The adopted peak ground acceleration and causal magnitude values are summarised in Table 5.1 below (with the exception of the Alpine Fault Rupture Scenario which is considered separately; see the discussion which follows).

Table 5.1: Seismic hazard PGA and Magnitude values adopted for this study. The Alpine Fault Rupture Scenario's return period is conditioned on the time that has elapsed since the most recent 1717 rupture.

Return Period	25-yr	Alpine Fault Rupture Scenario (approx. 30-yr, conditional)	50-yr	100-yr	250-yr	500-yr	1000-yr	2500-yr
Annual Exceedance Probability	4%	3%	2%	1%	0.4%	0.2%	0.1%	0.04%
PGA (g)	0.1 to 0.16	0.11 (16th percentile) 0.19 (50th percentile) 0.32 (84th percentile)	0.14 to 0.22	0.20 to 0.32	0.31 to 0.48	0.41 to 0.63	0.53 to 0.82	0.74 to 1.14
M_w	6.1 to 6.5	8.1	6.1 to 6.5	6.1 to 6.5	6.1 to 6.5	6.5 to 7.1	6.5 to 7.1	6.5 to 7.1
Seismic Source (km)[1]	62 to 17	55	60 to 17	57 to 17	54 to 17	50 to 17	46 to 17	41 to 17

Note 1. The site-to-source distance (e.g. distance from site to surface projection of fault plane) is used for the Gillins and Bartlett lateral spreading assessments and come from assessment of the distance to nearby faults

Glenorchy is located in between Queenstown (approximately 30km SE of Glenorchy) and Milford Sound (approximately 40km NW of Glenorchy). The PGA in Milford Sound is significantly greater than Queenstown (especially at longer return periods). Conversely M_W in Queenstown is greater than Milford Sound for the more frequent return periods. As a result, interpolation would result in considerable uncertainty and therefore for the upper bound values, the larger of the PGA and M_W values for Queenstown and Milford Sound have been combined, whereas for the lower bound values, the lower of two have been combined. The seismic hazard is typically the largest source of uncertainty and that the selected combinations were used to try and envelope the uncertainty.

The values in Table 5.1 (obtained from the Table A1 from Appendix A of the 2021 guidelines) are based on the 2002 National Seismic Hazard Model using the rupture reoccurrence intervals for each fault. However, neither the 2002 Model nor the updated NZGS/MBIE 2021 Module 1 Guidelines incorporate time dependency (i.e., elapsed time since the last earthquake). This means, based on the current understanding of the probability of an Alpine Fault rupture, the values in Table 5.1 are likely to be unconservative (excluding the ones for the Alpine Fault Rupture Scenario). The improved understanding of the Alpine Fault is currently not captured in the values presented in Table 5.1, which is significant since the Alpine Fault is likely to have a major contribution to the seismic hazard for Glenorchy.

To be more specific, the Alpine Fault has a relatively short rupture recurrence interval, estimated to be between 250 and 340 years. The Alpine Fault last ruptured in 1717 which means that 304 years have since elapsed. Because of this significant amount of time which has elapsed relative to the average (time-independent) recurrence interval, the time-dependent conditional probability of rupture is likely to be significantly shorter as shown by recent studies (Biasi, Langridge, Berryman, Clark, & Cochran, 2015); (Howarth, et al., 2021).

Moreover, recently published research (Howarth, et al., 2021) uses paleoseismic evidence to estimate a long-term time-independent recurrence interval of about 250 years, which is even lower than previous estimates of 300 to 340 years (N.B. Intervals between historical events have ranged from approximately 140 to approximately 510 years). Using this lower recurrence interval gives very high estimates of conditional rupture probability within the next 50 years; Howarth, et al. estimate this to be a 75% probability, with an 80% chance of it being an earthquake with a magnitude of 8 or above. A 75% probability of an Alpine Fault Rupture Scenario in the next 50 years is equivalent to an approximate conditional return period of 30 years.

Based on a deterministic calculation, the median PGA at Glenorchy for an Alpine Fault Rupture Scenario is 0.19g and the 16th and 84th percentile values are 0.11g and 0.32g. These estimates are based on a combination of Ground Motion Models (GMMs) with a 40% weighting assigned to the GMM developed by Bradley, et al. (Bradley, et al., 2017) and 20% weight assigned to each of three NGAWest2 GMMs (Abrahamson, Silva, & Kamai, 2013); (Boore, Stewart, Seyhan, & Atkinson, 2014); (Campbell & Bozorgnia, 2014).

These values have been tabulated in Table 5.1 under the Alpine Fault Rupture Scenario. It is noted that a 30-year return period event with a median PGA of 0.19g is a significantly higher than the published PGA values for the 25-year and 50-year return period events. This illustrates the unconservative nature of the values obtained from the 2021 NZGS & MBIE guidelines (which are based on the 2018 NZTA Bridge Manual values) which do not account for the time dependency of the Alpine Fault ruptures and are also based on older ground motion and source models (currently being updated by GNS). This update may well lead to the overall seismic hazard at Glenorchy for the range of return period levels of earthquake shaking being nearer the high side of the estimated range.

Howarth et al. estimate a 75% probability of occurrence of an Alpine Fault rupture within the next 50 years, which means that the next Alpine Fault rupture is almost certain to happen within current

planning horizons and is highly likely to trigger liquefaction (discussed in Sections 11 and 12) resulting in significant lateral spreading and ground surface subsidence. An Alpine Fault rupture earthquake will have a larger magnitude and therefore a longer duration. While liquefaction triggering is less sensitive to magnitude than it is to shaking intensity, in contrast lateral spreading is *more* sensitive, and larger magnitudes are likely to cause greater lateral displacements than the PGA and magnitude combinations from the 2021 NZGS & MBIE guidelines. As such, an Alpine Fault rupture scenario has also been considered for assessing the likely range of lateral displacements across Glenorchy.

6   Geology and Geomorphology

In addition to seismicity, the geology at Glenorchy plays an important role in assessing its liquefaction vulnerability. What follows is a detailed summary of the geological and geomorphological history of the location.

Sedimentation into the Wakatipu basin is estimated to have begun around 17,000 years before the present day. At that time, the Wakatipu Lake was larger than at present, with a prominent high-stand lake level at approximately 360mRL elevation (NZVD), inferred from well-preserved lake-edge terraces. This is around 50m higher than today; the lowering elevation can be attributed to a number of factors, but recently this has primarily been due to incision at the outlet.

Lake Wakatipu's outlet has changed since its formation after the last glacial maxim, but the present-day outlet (the Kawarau River) is thought to have captured the drainage during the last 10,000 years. The Kawarau outlet was incised through sediments and rock, resulting in a semi-progressive lowering of the lake level as this incision took place. The lake level stabilised between periods of lowering, and this formed further, lower lake terraces that are preserved in places on the present-day landscape. At least ten lake terraces have been mapped around the Glenorchy area.
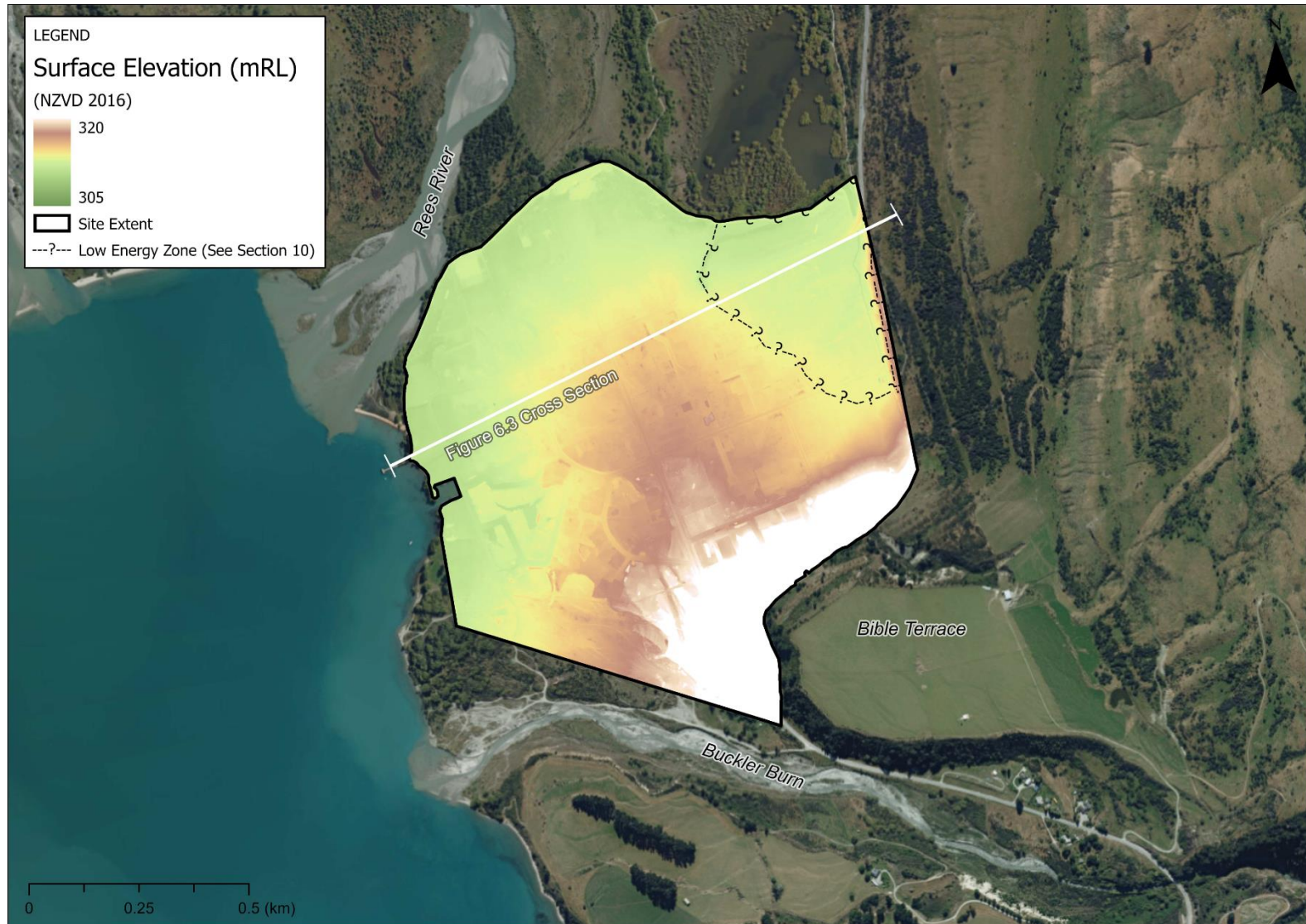
Figure 6.1: Surface elevation of Glenorchy, based on LiDAR survey. The location of the cross-section from Figure 6.3 is annotated. Elevations above 320mRL are truncated. The location of the low energy zone (discussed later in Section 10) is also annotated.

At a prominent lake high stand, the Buckler Burn formed what is now the Bible Terrace (annotated in Figure 6.1) and the terrace adjacent to Stone Creek. These terraces are part of the original Buckler Burn Fan/Delta complex which formed at the shoreline of the Lake when water levels were around 40m higher than today. The associated Alluvial Fan, Proximal delta topsets, and Gilbert Type delta foreset beds in distal deposits can all be observed in the river-cut exposures along the true left bank of the modern-day Buckler Burn (see Figure 6.2).

Figure 6.2: A photo of proximal delta topsets and Gilbert Type delta foreset beds in distal deposits in the river cut exposures along the true left bank of the modern-day Buckler Burn.

Along the western, lake-side edge of the township, it is likely that the building of the Bible Terrace Fan/Delta resulted in the accumulation of gently inclined fine silt sediment 'bottomset beds' on the lake floor sediments. These delta beds would conceivably dip north through west.

As the Lake Wakatipu water level lowered, the front of the Fan/Delta migrated around the edge of the existing fan, building out mainly westward. A comparatively deep lake basin, off the north edge of the Buckler Burn Fan/Delta (i.e., the north-east of the study area), seems to have had low sediment input during that time resulting in a lower energy deposition zone (shown in Figure 6.1). The top of the fan delta, which would now have been out of the water, became an alluvial fan with fluvial and alluvial modes of sediment deposition that created the present land surface there.

Once the lake had dropped to a level not much higher than the present day (estimated to be around 315–320mRL, NZVD) the Buckler Burn may have become entrenched as it eroded down through its fan delta, and flow was directed northward. This lake lowering is thought to have occurred in stages between about 5,000 and 500 years before the present day. During this time the Glenorchy township area appears to have been formed almost exclusively from sediment transported by the Buckler Burn, and so Glenorchy township is situated on the resulting lower fan delta complex.

During the building of this Glenorchy fan/delta, the Buckler Burn would have entered Lake Wakatipu several hundred metres from the current lake edge. The lake floor and bottomset sediments would probably have been overlain first by further bottomset type fine sediments at a low inclined angle northward, then by silt and fine sand dominated foreset beds which would have built out over the bottomsets as steeply inclined beds formed by finer sediments travelling down the delta front. The

foreset beds would probably have been emplaced as a series of overlapping lobes and the dip of the beds would likely be west through north to east and quite variable.

As the delta front migrated outward, toward the present-day Rees valley, a sharp transition would have been formed as proximal delta deposits (silt, fine to coarse sand and gravel) were emplaced in shallowing water over the top of the finer sediments. This transition is illustrated in a conceptual geological cross-section shown in Figure 6.3, and can be seen as the transition between the orange and yellow layers. The shallowing water would likely have been due to a combination of lowering lake levels and the filling of the available space within the basin by Buckler Burn sediments at the then lake margin. The coarse proximal delta deposits (topsets) would probably be low angled semi-braided channel deposited sediments gently dipping to the north and east. Similar deposits can be seen forming at the Rees and Dart deltas in the present day.
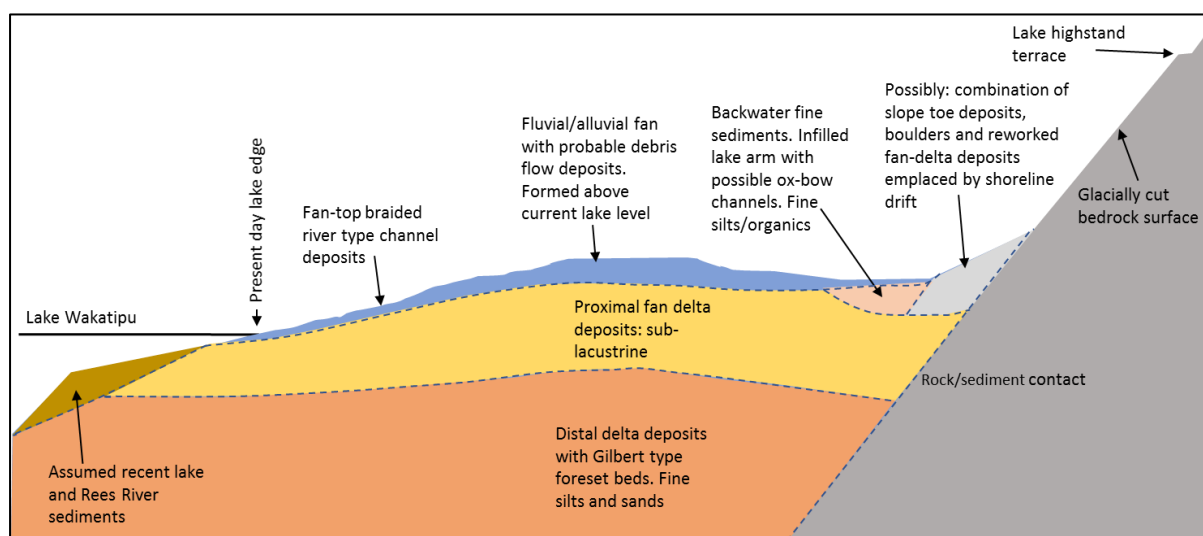

Figure 6.3: Informal, conceptual geological cross section (not to scale), at the location shown in Figure 6.1.

When the lake levels reached the present-day stand, fluvial and alluvial fan sediments (and probably debris flow deposits) from the Buckler Burn have overprinted on the Fan/Delta surface in fairly recent times forming a domed alluvial fan and many braided channels, especially on the western half of the Glenorchy township area. These coarse, generally gravel-dominated sediments vary in thickness between roughly 2m and 7m across the Glenorchy township, shown in the Figure 6.3 cross section in a blue colour. Deposition of these sediments seems to have ceased once the Buckler Burn became established in its present westward flowing channel.

Within the last 100–150 years it is likely that the Rees River delta has built out to connect with the Glenorchy fan/delta. The Rees River sediments are expected to onlap the Glenorchy delta front.

7 Topography

To undertake an assessment of liquefaction, and particularly lateral spreading, it is important to have a ground surface profile (including the surface of the lakebed underwater). For this study, a Digital Elevation Model (DEM) has been used. This DEM was derived from a LiDAR survey dating from 2019, provided by ORC, and illustrated in Figure 6.1. In addition, bathymetric data has been used (provided by NIWA via ORC) from a survey undertaken in Lake Wakatipu, likewise dating from 2019 (Survey RUK1901), using a Portable Hydrographic System.

Figure 7.1 shows a typical ground surface profile, together with a small map showing the line along which the profile is taken. There is a region near the edge of the lake where neither bathymetry nor LiDAR data is available (around point D); for this region an interpolation scheme was used based on

the slope (in each direction). In some areas further hydrographic survey data provided via ORC was available which validates this interpolation approach.
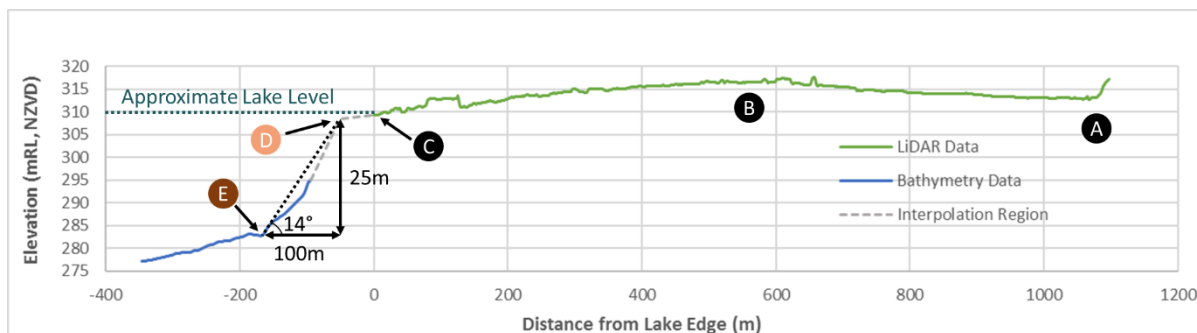

Figure 7.1: An example ground surface profile taken along the line shown in Figure 7.2. Note that the horizontal and vertical scales are not in a 1:1 ratio, so the vertical direction appears exaggerated. The significance of the points labelled A through E are explained in the text.

From point A (i.e., the foot of the ridge on the east side of Glenorchy), there is a gentle slope upwards for about 500m to point B, rising about 5m in elevation; at which point the highest elevation point is reached. Then, from point B there is a similarly gradual slope for about 600m down to point C, which corresponds to the edge of the lake, losing about 7m of elevation. The ground surface continues below the lake with a similar slope for about 50m to point D, at which point a significant drop-off begins: a vertical drop of about 25m over the span of 115m down to point E, at which point, the gradient of the slope eases off more.

For the purposes of a lateral spreading assessment, the drop-off starting at Point D is known as a *free face*. The edge of the free face (a.k.a. the crest) has been mapped along the lake edge (using the full Bathymetry and LiDAR data rather than a single cross section); shown in Figure 7.2. Likewise, the base of the free face (e.g., Point E in the cross section) has been mapped using a similar methodology.

Figure 7.2: The mapped free face crest location and base locations along the edge of Lake Wakatipu around Glenorchy, together with the line along which the surface in Figure 7.1 is taken. The crest and base intersect at points D and E from that figure, respectively.

Wherever significant liquefaction occurs, lateral spreading has the potential to occur on sloping land, and also flat land adjacent to free faces. At gently sloping sites, away from free faces, the lateral movement may be smaller, while sites adjacent to a free face, such as a riverbank or lake front, the movements can be larger and significantly more damaging. Damage is typically concentrated near to the free face and reduces with distance away from it.

The higher the free face, the larger the lateral spreading and the further back it extends. The free face height is up to 25m in this case, which is very significant. For comparison: following the Canterbury Earthquake Sequence, the areas that were most severely affected by lateral spreading in the residential red zone areas of Christchurch adjacent to the Avon River had free face heights of about 4m. Therefore, any lateral spreading in Glenorchy is likely to be more severe and extend much further back inland compared to the severity and extent of the lateral spreading observed in the residential red zone areas of Christchurch. Later, Section 13 explains this in further detail.

8 Geotechnical Investigations

Subsurface information from geotechnical testing is necessary to quantitatively assess liquefaction and its consequences. Accordingly, T+T engaged Geotechnics Ltd to carry out Cone Penetration Tests (CPT) and ProDrill Ltd to drill boreholes throughout Glenorchy township. These investigations were carried out during the week of 10–16 October 2021. T+T supervised the investigations, and an Engineering Geologist carried out a comprehensive walkover of the township and immediate surrounds to assess the geology and geomorphology of the area (see Section 6).

19 CPT were carried out, with a target depth of 20m. Of these, 11 CPT reached their target depth of 20 m and the remainder refused at shallower depths due to denser overlying gravels.

Four sonic boreholes were drilled. Two achieved a target depth of 20 m, and the other two were used to investigate and pre-drill the upper 7–8 m of medium dense gravelly sand, to enable CPT investigations at depth. SPTs were also performed for all four boreholes. While these boreholes and SPTs were not used directly for liquefaction vulnerability calculations, they provided important information to correctly interpret the CPTs and assist in the development of a geological model for the area (refer to Section 6).

The investigation locations are shown below in Figure 8.1, and the logs and data have been uploaded to the New Zealand Geotechnical Database (NZGD). Metadata, including the total test depth is shown in Table 8.1 for the CPT which were uploaded to the NZGD (one CPT was not uploaded due to data quality issues). The NZGD also contained six CPTs and one Borehole with SPT, all located at the historical site of the Mt. Earnslaw Hotel, and these are also shown in Figure 8.1. Note that in some cases multiple tests were carried out at the same location, so the multiplicity is not obvious on the map.

Table 3.3 of the MBIE/MfE Guidance (MBIE & MfE, 2017) guidelines specifies an indicative spatial density of 0.1 to 4 investigations per Ha for a Level C assessment. The spatial density of investigations undertaken for this study is about 0.2. While this is toward the lower end of the recommended density, because of the relatively uniform geology, there is not a very large spatial variability in the ground conditions, and it considered to be sufficient for a Level C assessment.

Figure 8.1: Geotechnical Investigation locations: data and logs available on the NZGD.

Table 8.1: Metadata for the geotechnical investigations available within the Glenorchy Study Region on the NZGD, including tests performed as a part of this study.

TTGD ID	Investigation Type	Test Depth	Reference ID	NZTM X	NZTM Y
BH_165999	Borehole	31.9	EGH-ENG21-BH01	1235186	5023260
BH_168505	Borehole	20.3	BH01	1235557	5023361
BH_168506	Borehole	20.3	BH02	1235507	5023126
BH_168507	Borehole	7.0	BH03	1235653	5023173
BH_168508	Borehole	7.6	BH04	1235751	5023214
CPT_166002	CPT	11.8	CPTu001	1235147	5023277
CPT_166004	CPT	20.0	CPTu001A	1235148	5023290
CPT_166006	CPT	1.4	CPTu002	1235233	5023259
CPT_166007	CPT	20.0	CPTu002A	1235232	5023262
CPT_166009	CPT	20.0	CPTu003	1235171	5023230
CPT_168486	CPT	3.0	CPT-P1b	1235339	5023174
CPT_168487	CPT	4. 6	CPT06a	1235271	5023258
CPT_168488	CPT	18.6	CPT-P2	1235479	5022865
CPT_168489	CPT	21.9	CPT08	1235117	5023199
CPT_168490	CPT	21.3	CPT02	1235897	5023615
CPT_168491	CPT	20.2	CPT01	1235983	5023652
CPT_168492	CPT	21.2	CPT03b	1235672	5023526
CPT_168493	CPT	22.0	CPT17	1235174	5022983
CPT_168494	CPT	20.2	CPT22b	1235658	5023178
CPT_168495	CPT	3.6	CPT20a	1235554	5023363
CPT_168496	CPT	20.0	CPT19a	1235513	5023473
CPT_168497	CPT	10.7	CPT10	1236104	5023373
CPT_168498	CPT	20.8	CPT13a	1235783	5023231
CPT_168499	CPT	21.1	CPT05a	1235348	5023286
CPT_168500	CPT	1.1	CPT15	1235503	5023129
CPT_168501	CPT	2.3	CPT16	1235233	5023033
CPT_168502	CPT	17.0	CPT04	1235467	5023331
CPT_168503	CPT	20.1	CPT12	1235905	5023267
CPT_168504	CPT	21.0	CPT18	1235403	5023720

9 Groundwater Model

A groundwater model was developed using data from monitoring for water quality purposes (e3 Scientific Ltd., 2018), together with the geotechnical investigations described in the previous section (Section 8).

Porewater pressure measurements for some CPTs were of a suitable quality to estimate a groundwater depth; this was converted to a groundwater elevation by subtracting from the LiDAR DEM surface. The monitoring well data reported by e3 Scientific (e3S) were already given in terms of elevation.

There were e3S monitoring well data available at the Glenorchy Jetty, the Lagoon, as well as nine other locations throughout the township. The mean well readings over a five-month period were used. The Jetty and Lagoon wells provide a boundary condition for the groundwater surface along the edge of the Lake and the Lagoon respectively (since the groundwater surface must be continuous with the water level). As such, the Lake was assumed to have elevation of 309.8mRL and the Lagoon; 311.0mRL (both NZVD).

While there was significant variability in the data, they supported a set of relatively gentle elevation contours increasing in the direction away from the lake. These contours are shown below in Figure 9.1.
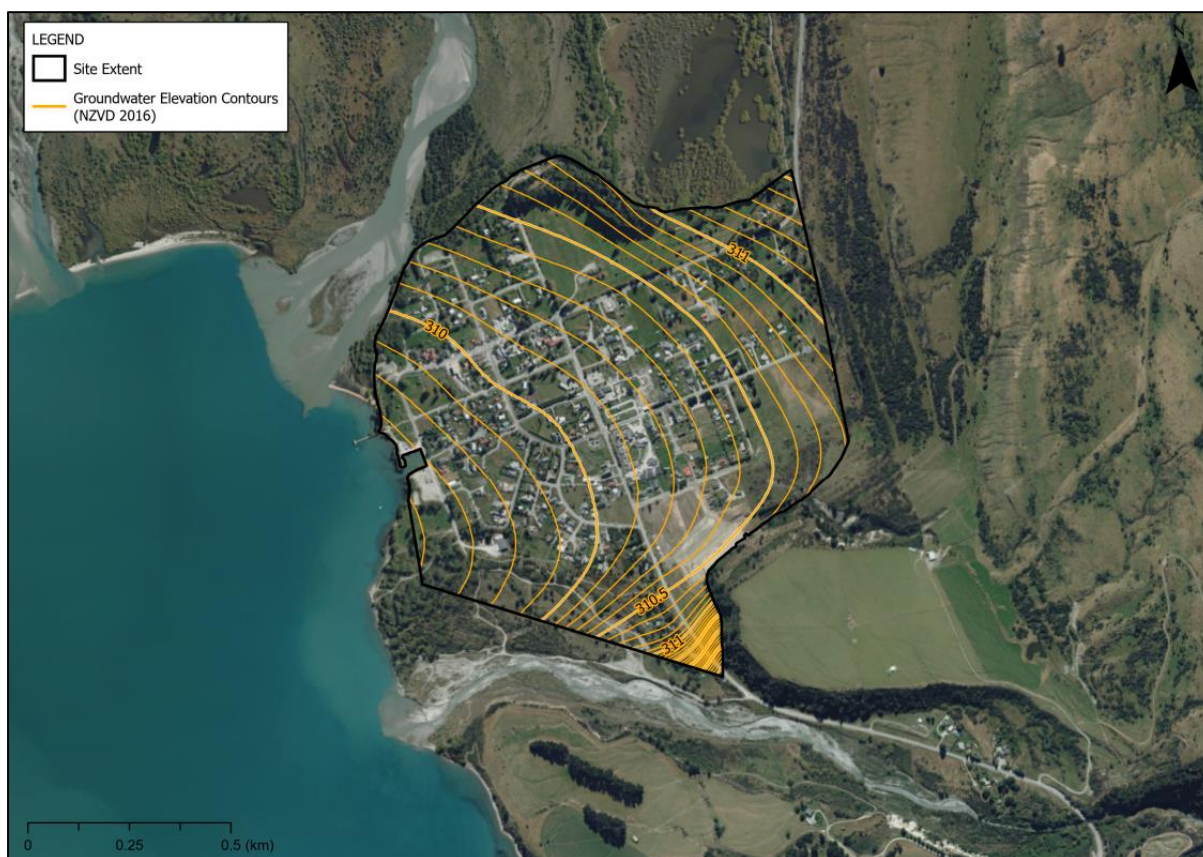

Figure 9.1: Contours for the groundwater surface model which has been developed for this study.

This Groundwater Elevation Model was then readily subtracted from the LiDAR DEM surface to give a Groundwater Depth Model, shown in Figure 9.2.
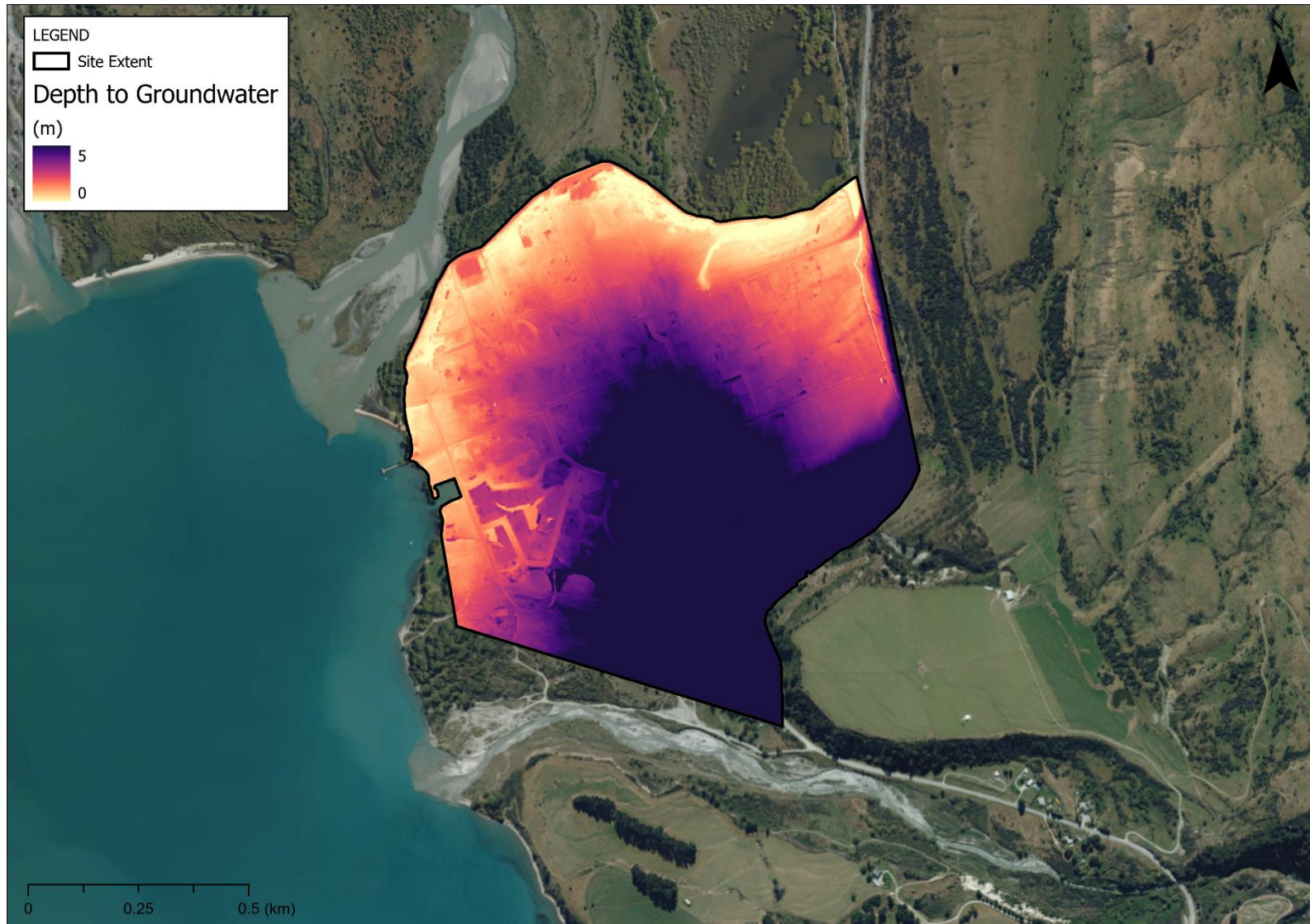
Figure 9.2: The modelled ground water depth for the study. Depths beyond 5m are truncated.

Due to the gentle slope in the groundwater surface, the groundwater depth is largely governed by the surface elevation (see Figure 6.1). The higher-elevation alluvial fan proceeding from Bible Terrace has deeper groundwaters, whereas near the lakefront, the lagoon, and in the north-east of the study area have significantly shallower groundwaters.

The e3S monitoring well data were collected during an exceptionally dry period, so the median groundwater could be higher. This would increase the liquefaction vulnerability, but not appreciably, as demonstrated later in Section 12 (in particular Table 12.3).

The groundwater model represents a possible, typical scenario for the purposes of a liquefaction vulnerability assessment. There is a certain level of seasonal variability which would be expected, and in time of flooding the lake and lagoon levels will be higher which will increase the groundwater levels. However, the probability of an earthquake occurring coinciding with elevated groundwater is very low, so for assessment of liquefaction and lateral spreading, the typical groundwater depths are more representative.

10 Ground Conditions

The geotechnical testing described in Section 8 were, in part used to develop the geological and geomorphological understanding presented in Section 6. Broadly speaking, there are two depositional environments in Glenorchy. Most of the study area has seen continuous deposition from the Buckler Burn and is has fairly consistent ground conditions apart from differences in soil unit layer thicknesses. The exception is the area off the north edge of the Buckler Burn Fan/Delta (i.e., the north-east of the study area), which seems to have generally seen lower levels of deposition, as evidenced in part by its depressed surface elevation; this region is annotated on the LiDAR DEM in Figure 6.1.

Following topographic contours and informed by the CPT data, which show the possible presence of organic silts in this low energy area, the north-east of the study area has been considered separately. The adopted boundary between the higher energy area and the lower energy area should be considered to have an uncertainty of approximately 100m either side of it, especially in the north near the Lagoon where CPTs are spaced further apart. This uncertainty could be reduced in the future through further subsurface geotechnical testing.

While the thicknesses and composition of layers varies throughout Glenorchy, a couple of general summaries of the subsurface conditions are provided for the high and low energy areas in Table 10.1 and Table 10.2 respectively. These correspond with the layers shown in the conceptual geological cross section in Figure 6.3.

In both the high and low energy zone, all strata below the Alluvial Fan Braided Channel Deposits consist of alluvial material, which is highly susceptible to liquefaction, beginning between about 3-7m below the ground but extending down to 20m and beyond. For comparison, these ground conditions are considerably worse than the ground conditions in the residential red zone areas of Christchurch where the thickness of highly susceptible material typically extended down to 10m below the ground surface.

Table 10.1: A general summary of subsurface conditions for the high energy area of Glenorchy (i.e., excluding the low energy zone shown in Figure 6.1).

Depth (m) (Approx.)		Unit	Generalized Description	Detailed Description	Typical CPT q_c and SPT N values	Figure 6.3 Cross Section Colouring
From	To					
0	0.3	Topsoil	Organic silt-sand	Organic silt-sand	N/A	N/A
0.3	4 to 7	Fluvial/Alluvial Fan and Fan-top Braided Channel Deposits	Gravels and Sands	Gravelly SAND to sandy GRAVEL. Medium dense to dense; well graded. Gravel is fine to course; subangular to subrounded, slightly weathered schist & quartz. Sand is fine to coarse. Silty CLAY (rare).	q_c typically 5–15MPa, occasionally higher: near 30MPa SPT N values of 13-20.	
4 to 7 (Only at Delta Edge)	5 to 10 (Only at Delta Edge)	Transitional Delta Edge Deposits	Interbedded Silts, Sands and Probable Gravels	Silty gravelly SAND; well graded to poorly graded; loose to medium dense. Silty CLAY; firm to stiff (occasional) Sandy GRAVEL; medium dense (occasional, below 12m).	q_c typically 1–10MPa	
5 to 10	19 to >22	Proximal Fan Delta Deposits	Sandy Gravel		q_c typically 5–15MPa SPT N values of 11-18	
19 to >22	>30	Distal Delta Deposits (Beds may be inclined)	Silts and Fine Sands		q_c typically 1–5MPa	

Table 10.2: A general summary of subsurface conditions for the low energy area of Glenorchy (shown in Figure 6.1).

Depth (m) (Approx.)		Unit	Generalized Description	Typical CPT q_c	Figure 6.3 Cross Section Colouring
From	To				
0	0.3	Topsoil	Organic silt-sand	N/A	N/A
0.3	2.5 to 3.5	Fan-top Braided Channel Deposits	Gravels and Sands	q_c typically 5–15MPa	
2.5 to 3.5	3 to 10	Backwater Fine Sediments	Silts, Fine Sands, Possible organic silt beds	q_c typically 1–5MPa	
3 to 10	6 to 13	Proximal Fan Delta Deposits, Transitional Distal Delta Deposits	Silts and Fine Sands (Beds may be inclined)	q_c typically 1–10MPa	
6 to 13	10 to >20	Distal Delta Deposits, Lake Deposits	Silt	q_c typically 1–5MPa	
10 to >20	>30	Possible Glacial Deposits or Bedrock	Rock	q_c > 50MPa	

11   Liquefaction Triggering

Liquefaction triggering at the site was assessed using the CPT data according to the methodology of Boulanger and Idriss (Boulanger & Idriss, 2014), as recommended by Module 3 of the NZGS/MBIE Earthquake geotechnical engineering practice guidelines (NZGS & MBIE, 2021b). Analysis was performed at using the 15th percentile cyclic resistance ratio equations and also the 50th percentile (median) equations.

Representative liquefaction triggering plots developed during the analysis are shown for three typical CPTs from the high energy zone (NZGD IDs 168502, 167503, and 16896) in Figure 11.1, Figure 11.2, and Figure 11.3; which correspond to a lower bound, upper bound, and Alpine Fault Rupture Scenario respectively. For the lower bound case, the lower bound PGA and M_W values from Table 5.1 were used, together with 50th percentile cyclic resistance ratio equations. For the upper bound case, the upper bound PGA and M_W values were used, and 15th percentile cyclic resistance ratio equations. Finally, for the Alpine Fault Rupture Scenario, the 50th percentile cyclic resistance ratio equations were used, but the three different PGA values in Table 5.1 were considered separately.

The silty gravelly SAND beginning at about 3 to 7m depth is mostly loose and the analysis shows it is highly susceptible to liquefaction. Of this material, the most susceptible zone is from about 5 to 12m depth. Below 12m the soil remains susceptible but there is a gradual increase in relative density with depth.

The upper crust from the surface down to 3 to 7m depth is considered unlikely to liquefy because it is significantly denser than the deeper soils and mostly above the ground water table.

The analyses show that triggering of liquefaction within the most susceptible zone (approx. 5 to 12m) is expected to occur when shaking intensity reaches a PGA of 0.13g. The remaining susceptible soils (approx. 12 to 20m and beyond) would likely liquefy with a PGA of 0.2g and above. The results indicate that soil liquefaction is significant and widespread across Glenorchy within these depth ranges and shaking intensity ranges.

Generally CPTs only reach 20m and the simplified liquefaction triggering assessment methodologies (Boulanger & Idriss, 2014) are only applicable for the top 20m; it is probable that liquefaction could trigger at depths below 20m, so for the upper bound case, the CPTs shown have been extrapolated. The extrapolation was performed using uniform values of q_c = 8.5MPa and I_c = 1.9, which correspond to the median values for available CPT data in the study region over the depth ranges of both 15-20m and 20m+.

Figure 11.1: A plot of lower bound liquefaction triggering (and the resulting cumulative thickness) at increasing return period levels of earthquake shaking, for three representative CPTs from the high energy area.
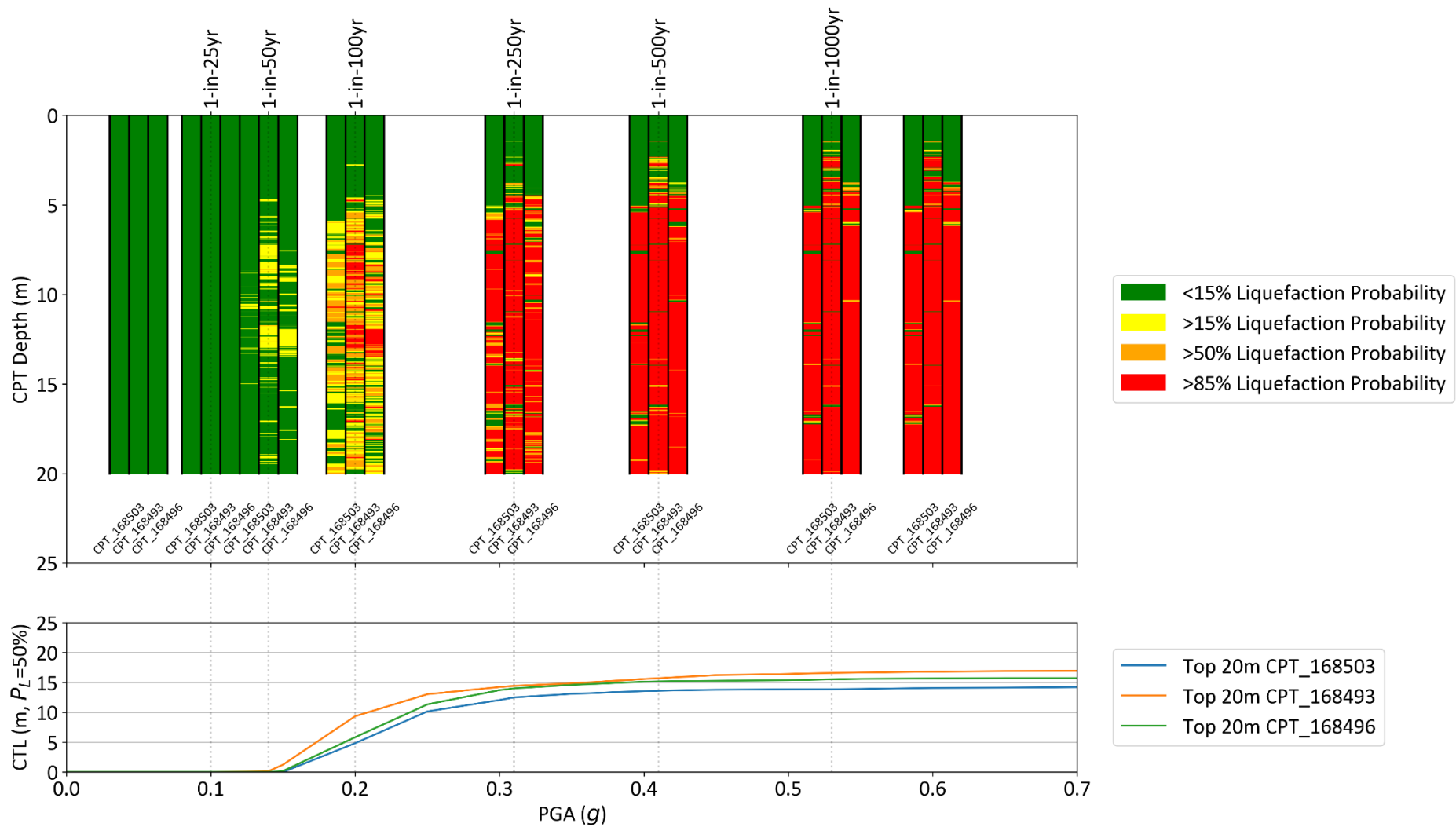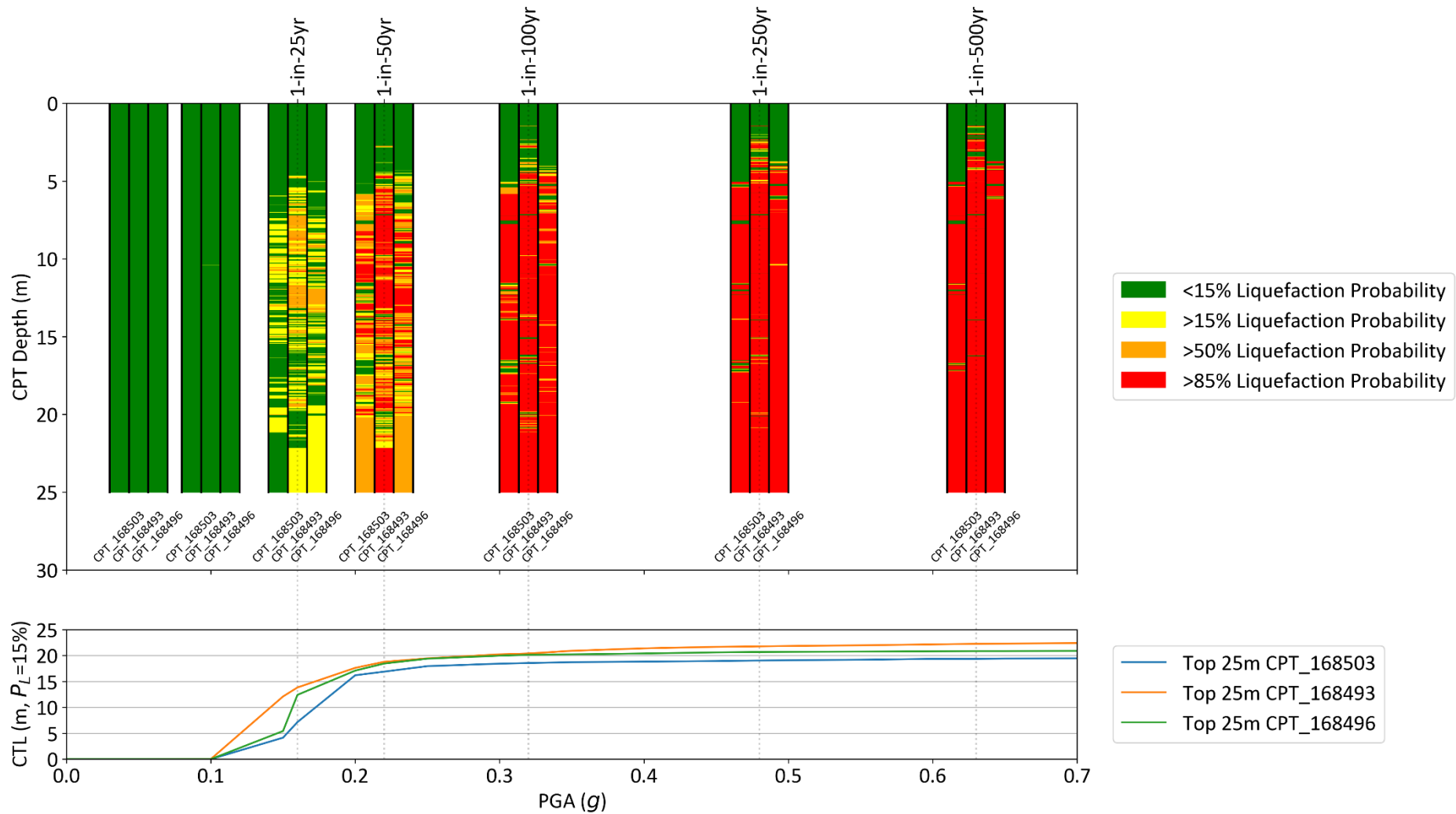
Figure 11.2: A plot of upper bound liquefaction triggering (and the resulting cumulative thickness) at increasing return period levels of earthquake shaking, for three representative CPTs from the high energy area.
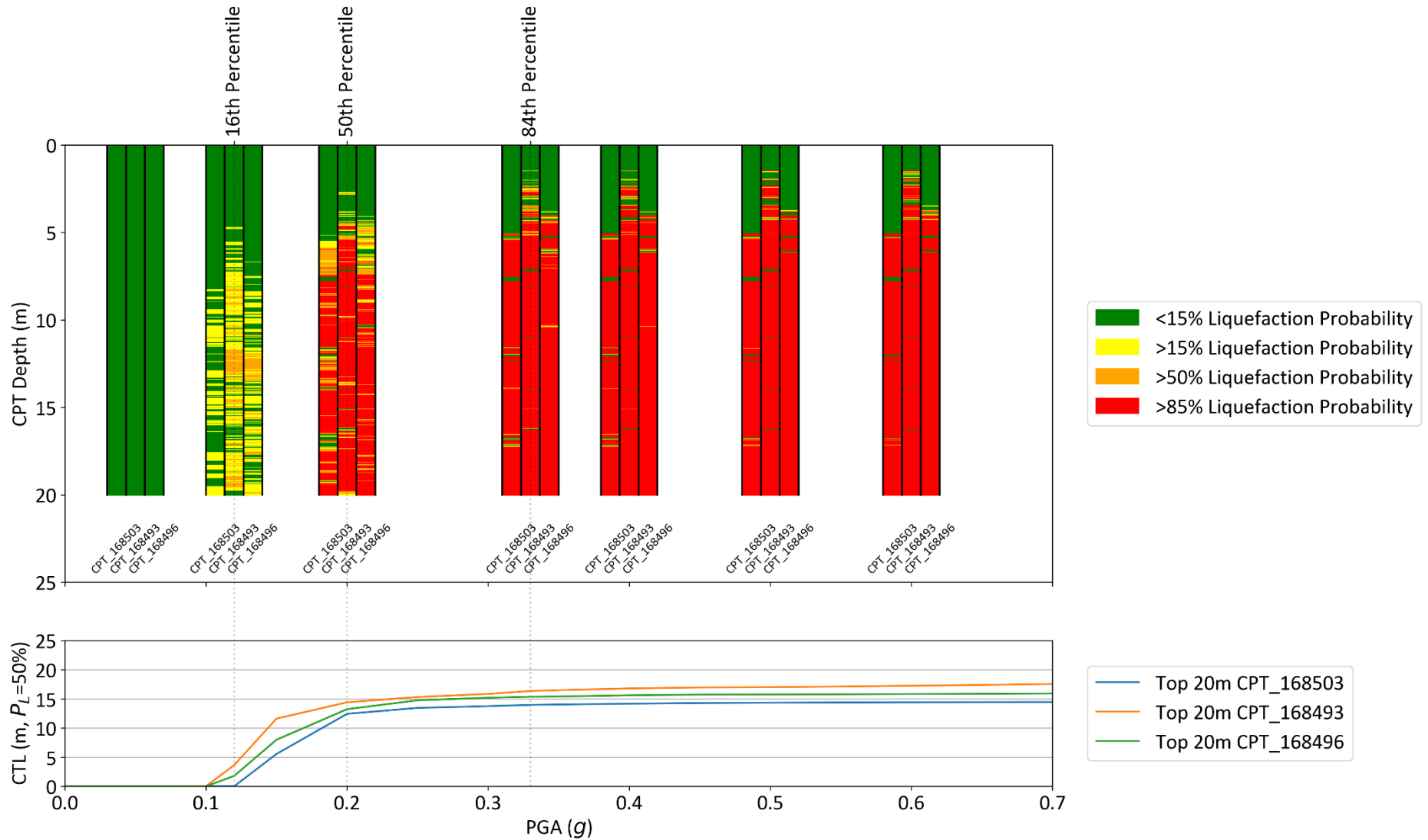
Figure 11.3: A plot of liquefaction triggering for an Alpine Fault Rupture Scenario (and the resulting cumulative thickness) for the 16th, 50th and 84th percentile shaking levels, for three representative CPTs from the high energy area.

The results shown in Figures 11.1 to 11.3 show that for the higher levels of earthquake shaking between 15 to 20m of the soil profile is predicted to liquefy for the three selected CPT. The liquefaction triggering is initiated at 25 to 50-year return period levels of earthquake shaking and is fully developed at the 50 to 100-year return period levels of earthquake shaking. Higher levels of shaking at higher return periods do not significantly increase the thickness of the soil layers that are likely to liquefy. For the Alpine Fault Rupture Scenario, liquefaction triggering is predicted for the 16th, 50th and 84th percentile ground motions. This means that for an Alpine fault scenario, despite the uncertainties in the shaking intensities likely to occur at Glenorchy, liquefaction triggering is likely.

Tables 11.1 and 11.2 visually show the predicted thickness of the Cumulative Thickness of Liquefaction (CTL) for the deep CPTs for the lower bound, upper bound cases (Table 11.1), and Alpine Fault Rupture Scenario (Table 11.2) respectively. The three CPTs from Figure 11.1, Figure 11.2, and Figure 11.3 (NZGD IDs 168502, 167503, and 16896) are annotated as *A*, *B*, and *C* respectively in the figures in Table 11.1 and 11.2.

As mentioned in the previous section (Section 10); for comparison the thickness of liquefiable material is greater (approximately double) compared to the worst performing residential red zone land in Christchurch.

The low energy zone (see Figure 6.1) has a significantly higher presence of clayey silts in the 5 to 12m range, compared to the high energy zone. Whereas in the high energy zone this is the most susceptible range, in the low energy zone there is significantly more variability, mostly due to the variability in silt versus clay/organic content, rather than due to differences in density. CPT_168497 in the eastmost side of Glenorchy has a significant amount of sensitive, fine-grained material which is assessed as less susceptible compared to the other two CPTs in the area, which instead have more silty material throughout. Further CPTs in the area would help to reduce the uncertainty associated with this spatial variability.

Table 11.1: The cumulative thickness of liquefaction at each CPT for various return periods, for both the lower bound case (top row) and the upper bound case (bottom row). NZGD CPTs 168502, 167503, and 16896 are labelled as A, B, and C respectively.

Cumulative Thickness of Liquefaction

- 🟢 Less than 2m
- 🟢 2–5m
- 🟡 5–10m
- 🟠 10–15m
- 🔴 15–20m
- 🔴 20–25m
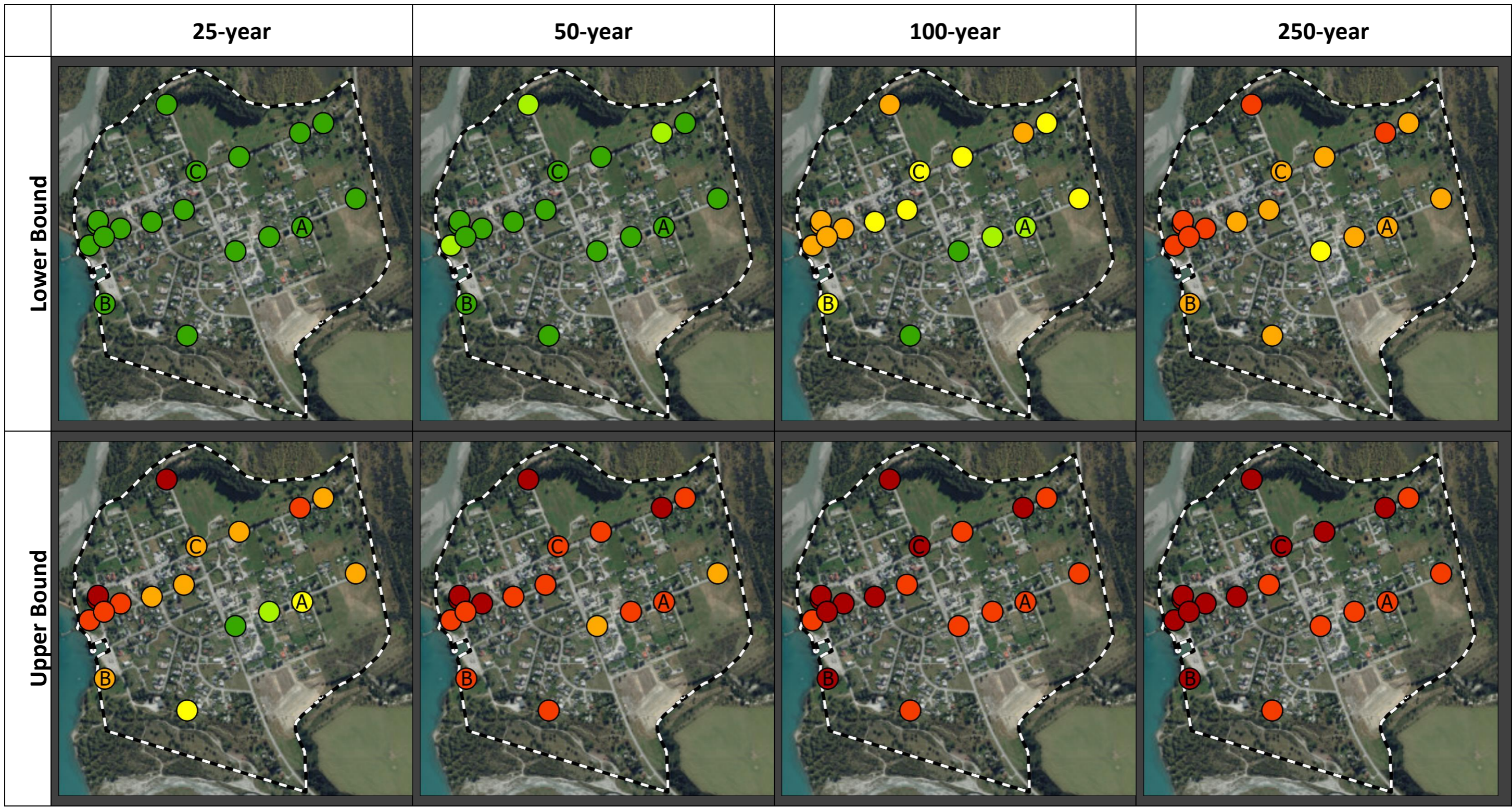
Table 11.2: The cumulative thickness of liquefaction at each CPT for the Alpine Fault Rupture Scenario for the 16th, 50th and 84th percentile shaking estimates. NZGD CPTs 168502, 167503, and 16896 are labelled as A, B, and C respectively.

16th Shaking Percentile	Median Shaking	84th Shaking Percentile

Cumulative Thickness of Liquefaction

- 🟢 Less than 2m
- 🟢 2–5m
- 🟡 5–10m
- 🟠 10–15m
- 🔴 15–20m
- 🔴 20–25m
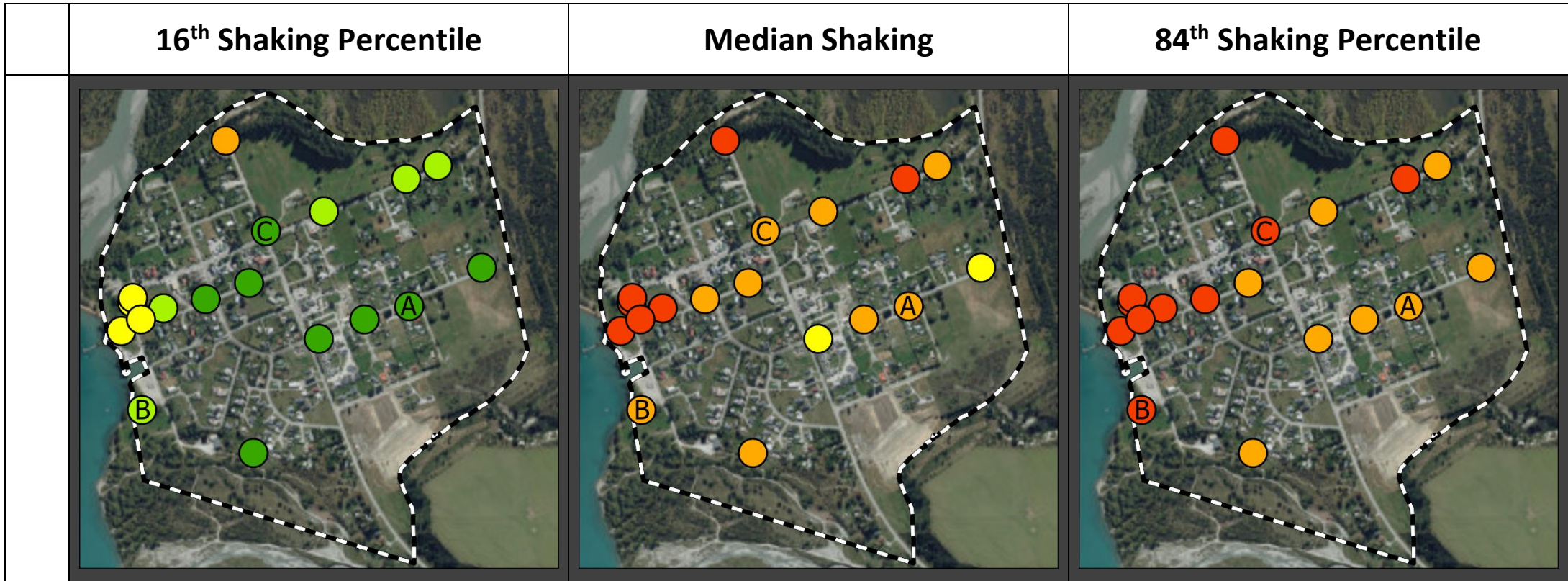
12   Liquefaction Land Damage Model

There are significant and widespread subsurface soil layers where liquefaction is likely to trigger. To understand what a realistic liquefaction scenario might look like with these ground conditions, a spatially probabilistic liquefaction land damage model (ignoring the effects of lateral spreading effects on the lake side of Glenorchy) has been developed. Note the lateral spreading effects are assessed separately (refer to Section 13). This was deemed necessary since within each geological layer there was no apparent spatial trend to the varying CPT tip resistance values used to infer the relative density of the material. In other words, the variability in relative density in each geological layer was found to be randomly distributed spatially within the Glenorchy area. Therefore, calculating liquefaction land damage indices at each CPT location and then interpolating the results could result in misleading outcomes necessitating the need to utilise a spatial probabilistic approach.

CPT and Borehole logs were used to establish the thicknesses of different geological layers as a continuous surface across Glenorchy. Then, the liquefaction triggering methodology (Section 11) was used to determine vertical settlement strain due to liquefaction-induced volumetric consolidation for each geological layer.
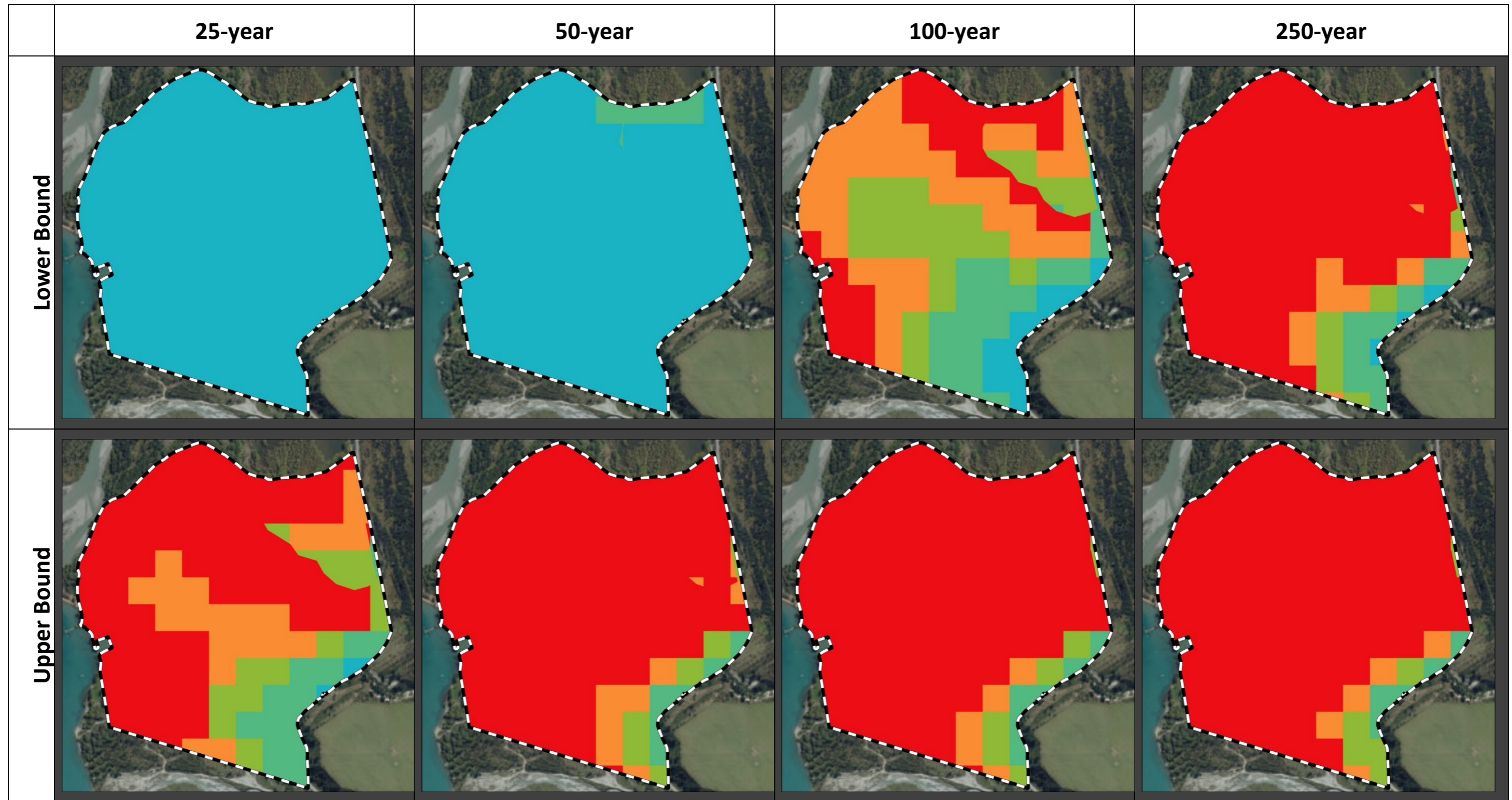
These volumetric strain values for each CPT were used to fit a probabilistic distribution for the volumetric strain for each geological layer separately. This was repeated for the range of return period earthquakes listed in Table 5.1. Then, the study area was divided into a grid of 100m-by-100m cells representing areas which have statistically independent volumetric strains. Volumetric strains were then sampled from the probabilistic distributions for each geological layer separately to calculate the corresponding liquefaction severity numbers (LSNs), giving a simulated, possible realization of liquefaction land damage across the study area.

LSN values of 0 to 8 correspond to none to minor liquefaction land damage, values of 8 to 16 correspond to minor liquefaction land damage, values of 16 to 20 correspond to minor to moderate liquefaction land damage, values of 20 to 25 correspond to moderate to high liquefaction land damage and values greater than 25 correspond to high to severe liquefaction land damage. Examples of the type of liquefaction land damage that can be expected when LSN values are greater than 25 are shown in Figures B10, B11 and B12 in Appendix B.

The median LSN over a large number of simulations is mapped in Table 12.1 for the lower bound and upper bound cases for a range of return periods. Similarly, the median LSN over a large number of simulations is mapped in Table 12.2 for Alpine Fault Rupture Scenario for the 16th, 50th and 84th percentile ground motions. Note that once the shaking is high enough, the additional liquefaction resulting at higher levels of shaking is negligible (as shown in Figure 11.1, Figure 11.2, and Figure 11.3) so the 250-year event case is considered to be representative of larger earthquakes for the lower bound case and the 50-year event case is fairly representative of larger earthquakes for the lower bound case. For the Alpine Fault Rupture Scenario, the results at the 50th and 84th percentile shaking levels are similar, whereas the at the 16th percentile shaking levels the liquefaction damage is considerably less severe.

These maps of liquefaction show that severe liquefaction land damage can occur at earthquake shaking levels as low as 25-year return periods. Between 25 and 100-year return period levels of shaking the liquefaction land damage becomes far more significant and widespread across all the lower lying areas of Glenorchy in the north and west (similar to what is shown in Figures B10, B11 and B12 in Appendix B). It is very important to understand that these maps show an estimate of the median performance over many possible scenarios; however in reality there would likely be areas where the liquefaction is more severe than the median, as well as areas where it is less severe. This is an inherently probabilistic process and these maps are intended to show broad trends across Glenorchy. The maps should not be used as a basis for site-specific assessment for any particular site.

Table 12.1: The median LSN from a large number of simulations for various return periods, for both the lower bound case (top row) and the upper bound case (bottom row).

Liquefaction Severity Number (Median Across Simulations)

- 0–8 (None to Minor)
- 8–16 (Minor)
- 16–20 (Minor to Moderate)
- 20–25 (Moderate to High)
- 25+ (High to Severe)

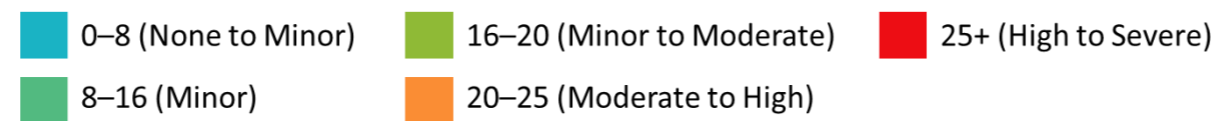*Table 12.2: The median LSN from a large number of simulations for various return periods, for the Alpine Fault Rupture Scenario.*

16th Shaking Percentile	50th Shaking Percentile	84th Shaking Percentile

Liquefaction Severity Number (Median Across Simulations)

- 0–8 (None to Minor)
- 8–16 (Minor)
- 16–20 (Minor to Moderate)
- 20–25 (Moderate to High)
- 25+ (High to Severe)
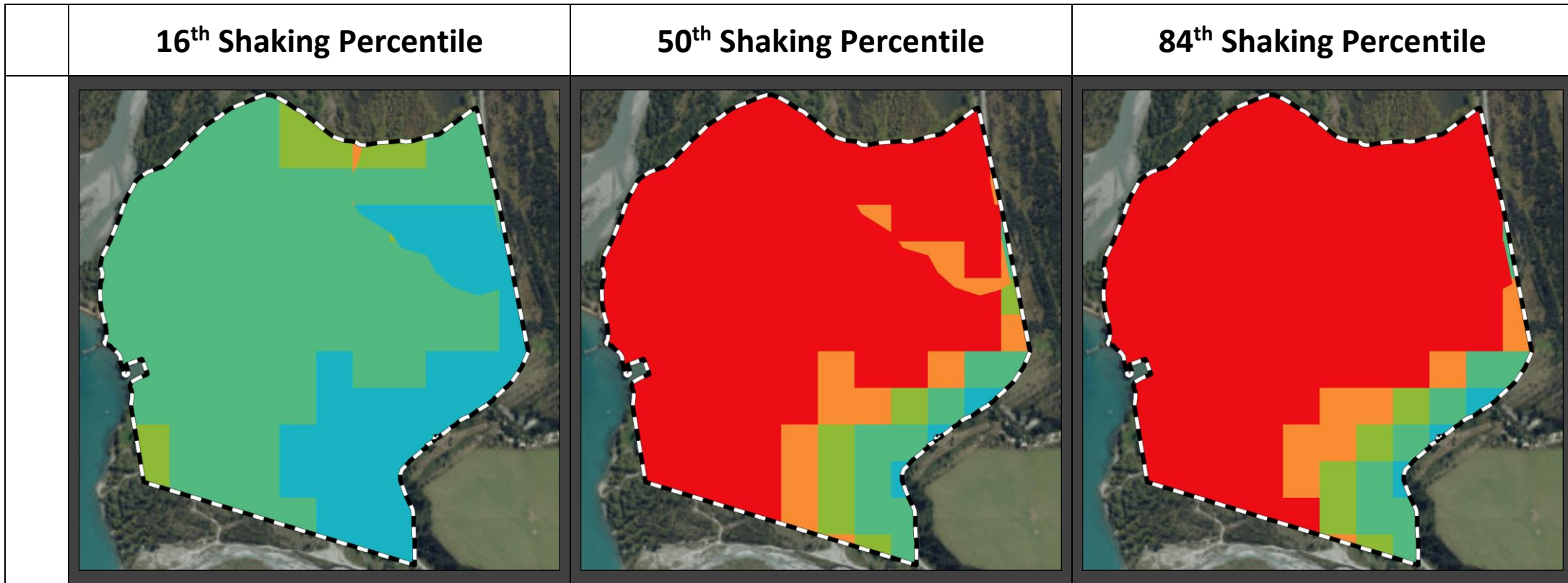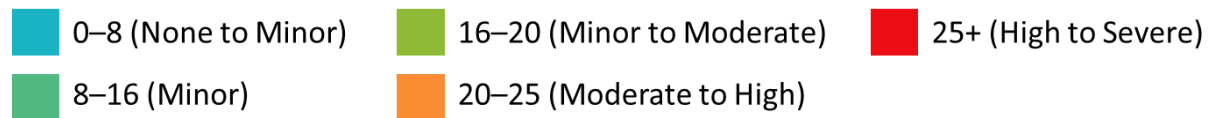
As noted in Section 9, the data used to develop the groundwater model was collected over an exceptionally dry period, so the median groundwater could potentially be higher. Table 12.3 shows the results of a sensitivity analyses of a 1m groundwater rise on the liquefaction vulnerability model for the lower bound case. It demonstrates that the increase in liquefaction vulnerability is not appreciable for most of the Glenorchy study area, indicating that the liquefaction vulnerability model is not particularly sensitive to uncertainty in the groundwater levels. The exception is in the northeast where there is an increase in liquefaction vulnerability with higher ground water levels at the more frequent return periods.

Table 12.3: A comparison of the median LSN (for a large number of simulations) showing the effect of a 1m groundwater rise for the lower bound case, for various return periods.
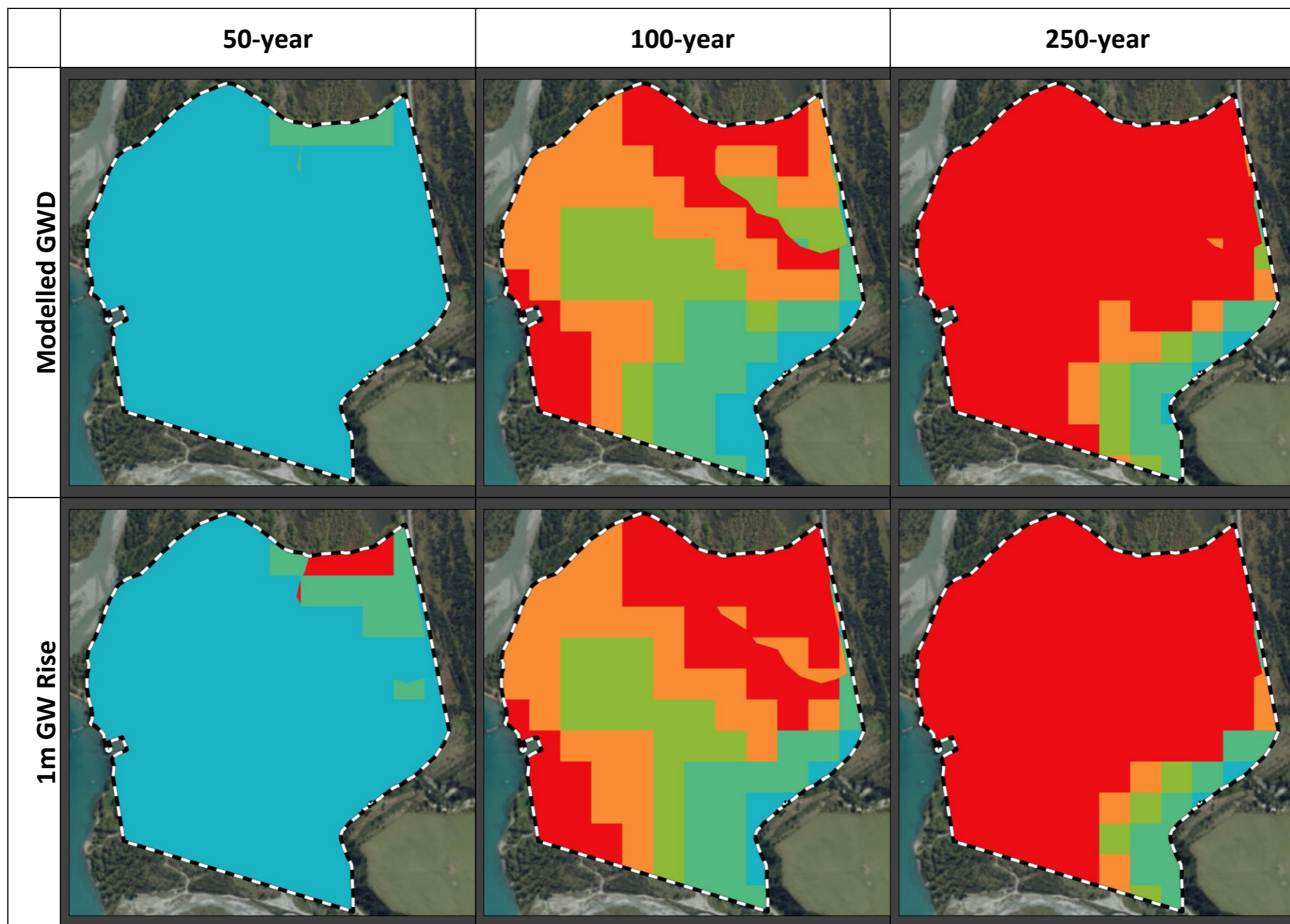
Liquefaction Severity Number (Median Across Simulations)

- 0–8 (None to Minor)
- 8–16 (Minor)
- 16–20 (Minor to Moderate)
- 20–25 (Moderate to High)
- 25+ (High to Severe)

13 Lateral Spreading Assessment

13.1 1D Lateral Spreading Assessment

Methods for estimating lateral spreading displacements at the site exist but these are known to have limited accuracy (typically the accuracy of predictions has been shown to be within a range of half to double when compared to the observed lateral spreading). Three methods have been used to assess the lateral spreading for both the lower and upper bound cases to understand the expected displacements that can be expected at the various return periods. The three methods that have been used are:

- The semiempirical approach proposed by Zhang et al. (Zhang, Robertson, & Brachman, 2004);
- The empirical equation proposed by Gillins & Bartlett (Gillins & Bartlett, 2014) has been adopted, which is a modification of an earlier equation proposed by Youd et al. (Youd, Hansen, & Bartlett, 2002); and
- The flexible sliding block method (Newmark block type assessment) proposed by Bray and Macedo (Bray & Macedo, 2019).

The Bray & Macedo method has a lot of steps and is time consuming to apply. At each offset distance from the lake new stability modelling is required to assess the lateral spreading at that point. Therefore, the Bray & Macedo method has only been applied for a limited extent as an independent check of the lateral spreading predicted by the other two methods with are much simpler and less time consuming to apply.

The lateral spreading assessments were undertaken for the typical cross section shown in Figure 7.1 and 7.2. The results are shown in Figure 13.1 for the upper and lower bound case, and in Figure 13.2 for the Alpine Fault Rupture Scenario. The analysis was performed at different offsets from the lake edge; in the case of the methodology proposed by Bray & Macedo (2019), the analysis has only been performed to approximately 140m from the lake edge.

The results for the Zhang et al. (2004) method are shown on the left-hand column, the results from the Gillins & Bartlett (2014) method are shown in the middle column and the results from the Bray and Macedo (2019) method are shown on the right hand column. For Figure 13.1 the top row is for the 25-year return period levels of earthquake shaking, and the bottom row is for the 500-year return period levels of earthquake shaking. The results for the lower bound case for each method for each return period are denoted by the lower bound dashed line in each graph and the results for the upper bound case for each method for each return period are denoted by the upper bound dashed line in each graph. The shading in-between the lower and upper bound lines represent the likely range of displacement predicted by each method. It is noted that the lower bound lateral spreading estimates are zero for return period levels of earthquake shaking of 25 years for the Zhang et al. method, 50 years for the Bray and Macedo method and 250 years for the Gillins and Bartlett method. The credibility of these lower bound estimates, in particular for the Gillins at Bartlett method, are discussed below.
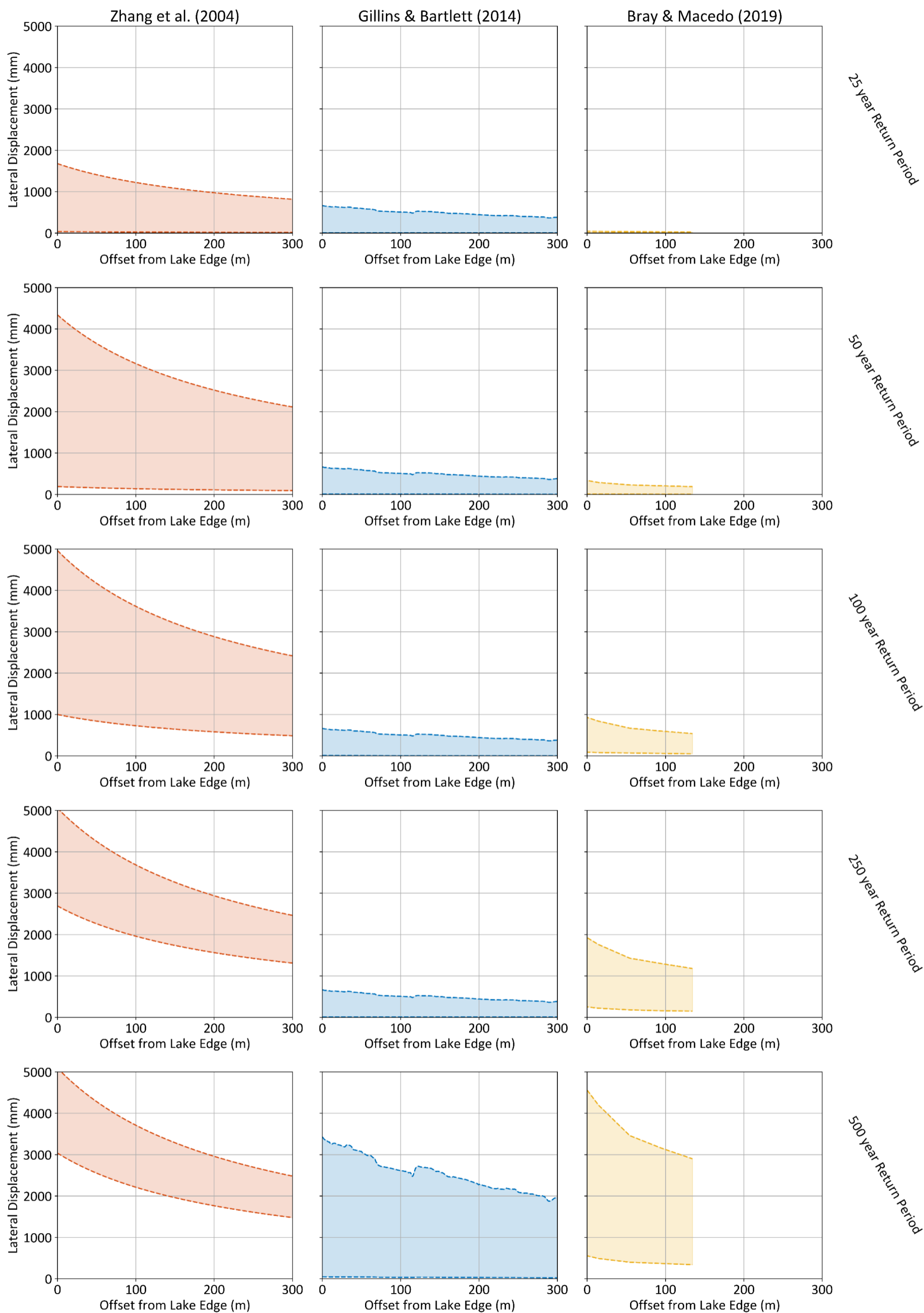
Figure 13.1: Lateral Spreading versus the distance from the Lake Edge for a representative cross section, comparing three different assessment methodologies (across columns) and different return-periods (across rows). On each graph, the upper dashed line represents the upper bound case, and the lower dashed line represents the lower bound case.
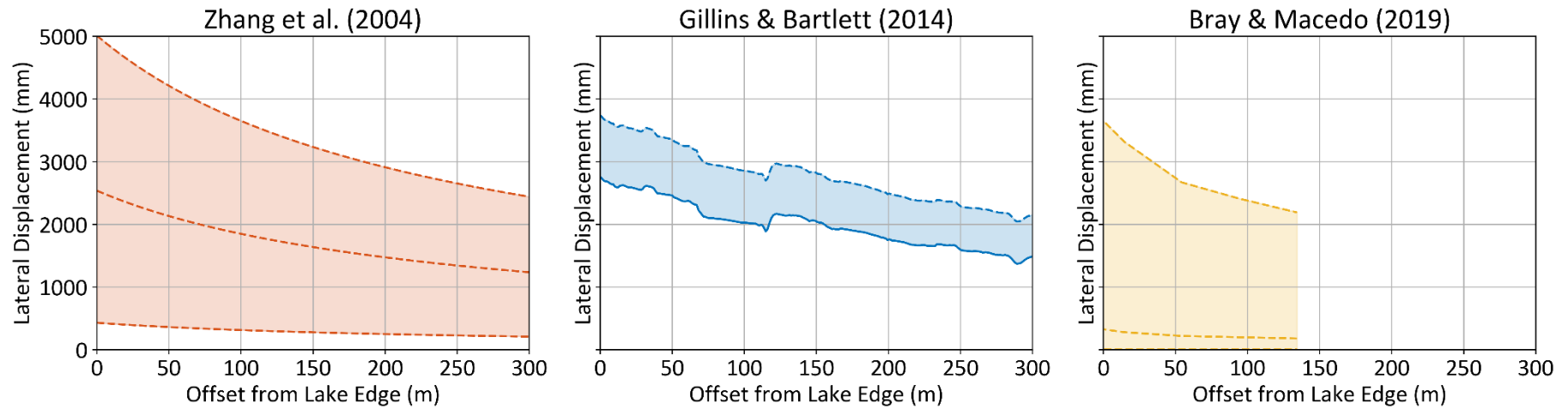
Figure 13.2: Lateral Spreading versus the distance from the Lake Edge for a representative cross section for the Alpine Fault Rupture Scenario, comparing three different assessment methodologies (across columns). For the method given by Zhang et al. there are three dashed lines corresponding to the 16th, 50th, and 84th percentiles of shaking. For that given by Gillins & Bartlett (2014), the 16th and 50th lines coincide as a solid line, whereas the 84th line is dashed. Finally, for the method given by Bray & Macedo (2019), the 16th line is approximately zero, while the 50th and 84th lines are shown as dashed.

The results for the typical cross section show:

- The lateral spreading is highest near the lake edge and decreases with increasing distance from the lake edge – as would be expected;
- The lateral spreading increases with larger return period earthquake shaking. At the 25-year return period levels of earthquake shaking the lateral spreading is likely to be less than 1m at the lake edge whereas at 500-year return period levels of earthquake shaking the lateral spreading could be up to 4 to 5m (typically twice as large as the lateral spreading that was observed in the residential red zone of Christchurch following the 2010 to 2011 Canterbury earthquakes – refer to Figures B1, B4, B5, B6, B7, B8 and B9 in Appendix B);
- The lateral spreading from an Alpine Fault Rupture Scenario is likely to be similar to the lateral spreading from 500-year return period levels of earthquake shaking (i.e. 3 to 5m at the lake edge);
- The different methods estimate different ranges of lateral spreading, particularly at the more frequent return periods. The estimates from the different methods become more consistent at the larger return periods and also for the Alpine Fault Scenario;
- The range of lateral spreading estimates obtained using the Gillins & Bartlett (2014) method are mostly within the same range given by the Bray and Macedo (2019) method up to 250-year return period levels of earthquake shaking; and
- The results using the Zhang et al. (2004) method generally indicate higher lateral spreading estimates and conversely the results using the Gillins & Bartlett (2014) method generally indicate lower lateral spreading estimates.

While each of the methods shows similar trends, the different methods result in a different range of lateral spreading predictions. They are all valid models and they each have technical strengths and weaknesses. They have been derived or validated against international case histories of lateral spreading from historical earthquakes. Therefore, to obtain an upper bound lateral spreading estimate, each method has given an equal weighting (i.e., a 33% weighting to each method).

It is noted that the upper bound weighted average lateral spreading estimate for the 500-year levels of shaking is approximately 1.2 times the upper bound Gillins & Bartlett (2014) method results.

For the Gillins & Bartlett (2014) method the lower bound estimates for the larger return periods indicate no lateral spreading. This is unrealistic but can be explained by the higher seismic source distances in Table 5.1 for the lower bound case. The Gillins & Bartlett (2014) method does not use shaking intensity as input variable, but instead uses the earthquake magnitude and seismic source distance[1]. However, at the larger return periods, even for the lower bound case shaking levels, liquefaction triggering *is* predicted using the methodology in Section 11. Therefore, the lower bound estimates for the Gillins & Bartlett (2014) method are not considered credible at the larger return periods. Hence, to develop a lower bound lateral spreading estimate, the Gillins & Bartlett (2014) method has been given a zero weighting, while the other two methods an equal weighting (i.e., a 50% weighting to each method).

It is noted that the lower bound weighted average lateral spreading estimate for the 500-year levels of shaking is approximately 0.5 times the upper bound Gillins & Bartlett (2014) method results.

For the Alpine Fault Scenario, the 16th percentile estimates from the Gillins & Bartlett (2014) method are higher than the lower bound estimates for a (time-independent) 500-year Return Period. This is because of the larger magnitude for that scenario.

---

[1] In other words, there is, embedded into the empirical equations, a simplified ground motion prediction allowance, which at larger seismic source distances results in negligible shaking intensity and hence negligible lateral spreading for the smaller earthquake magnitudes.

It is noted that the 84th percentile weighted average lateral spreading estimate for the Alpine Fault Scenario is approximately the 1.0 times the 84th percentile Gillins & Bartlett (2014) method results (i.e., they are approximately equal).

13.2   2D Lateral Spreading Assessment

The results from the 1D lateral spread assessment described in Section 13.1 have been used to develop and calibrate a 2D lateral spread assessment to enable the development of lateral spread contours for the 500-year levels of shaking as well as the Alpine Fault Scenario.

The Gillins & Bartlett (2014) method was used to develop lateral spread contours across the entire western side of Glenorchy in 2D at points in a 1m x 1m grid. The distance to the nearest point on the free face (mapped in Figure 7.2) was determined for each grid point, and the effective free face height was determined based on the maximum depth of predicted liquefaction (according to the assessment in Section 11), along with the cumulative thickness of liquefiable material. Lateral spread calculations were then performed at each grid point using these inputs, along with the seismicity information from Table 5.1.

To obtain an estimate for lateral spreading at a 500-year return period, the Gillins & Bartlett (2014) values have been scaled based on the analyses and results discussed in Section 13.1. In particular, to develop upper bound lateral spreading contours, the upper bound estimate from the Gillins & Bartlett (2014) method were scaled by a factor of 1.2. To develop lower bound lateral spreading contours, the upper bound estimate from the Gillins & Bartlett (2014) method were scaled by a factor of 0.5. The lower bound and upper bound estimates are shown in Table 13.1. The lateral spreading estimates range from 0.5m (lower bound) to 4m (upper bound) at the lake edge.

Similarly, for the Alpine Fault Rupture Scenario, the 84th percentile lateral spread values were determined as 100% (i.e., the same) as the Gillins & Bartlett (2014) values. For the 50th and 16th percentile, scaling factors of 50% and 0% have been applied respectively. The 16th, 50th and 84th percentile lateral spreading contours for the Alpine Fault Scenario are shown in Table 13.2. The lateral spreading estimates range from 0 metres (16th percentile) to 3 metres (84th percentile) at the lake edge.

For context, the lateral spreading that occurred in the worst performing land in Christchurch (which subsequently became the residential red zone) was typically in the order of 1 to 3m. Therefore, based on Table 13.1, the predicted lateral spreading near the lake in Glenorchy for the 500-year return period levels of shaking is comparable or worse to that observed in the worst parts of the residential red zone in Christchurch (refer to photos B4 to B9 in Appendix B).

The higher the free face, the larger the lateral spreading and the further back it extends and the more potential damage at any given distance (i.e., greater displacements). As already discussed in Section 7, the free face height is 25m in this case, which is significant. Following the Canterbury Earthquake Sequence, the areas that were most severely affected by lateral spreading in the residential red zone areas of Christchurch had free face heights of about 4m. Consequently, the lateral spreading damage is likely to be more severe compared to the residential red zone areas of Christchurch and also likely to extend further inland and hence be more extensive compared to the extent of the residential red zone areas of Christchurch.

Table 13.1: Lateral Spreading for the lower bound and upper bound cases. The ground would be expected to move towards the lake by the annotated distance.

	Lower Bound	Upper Bound
500-year Return Period		

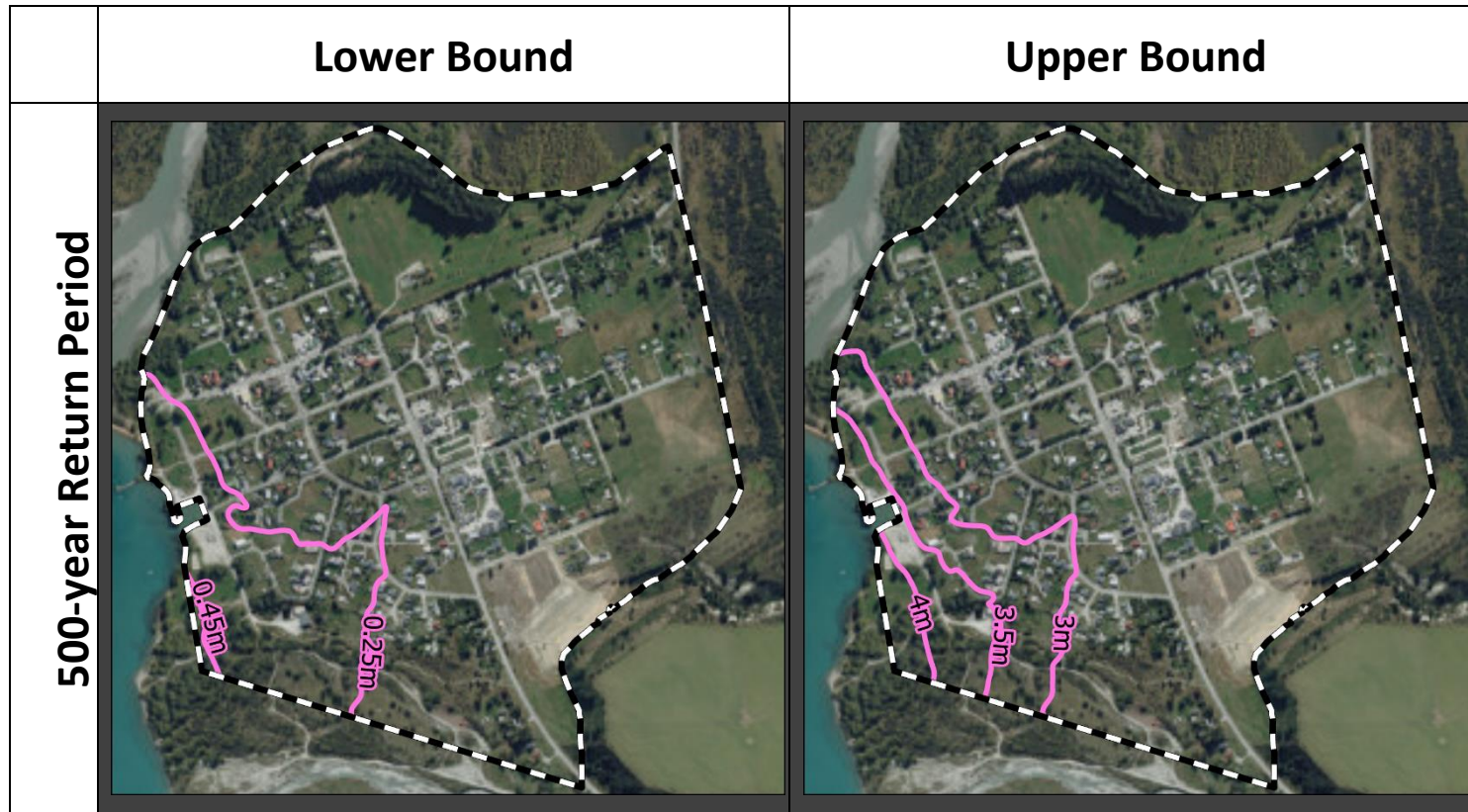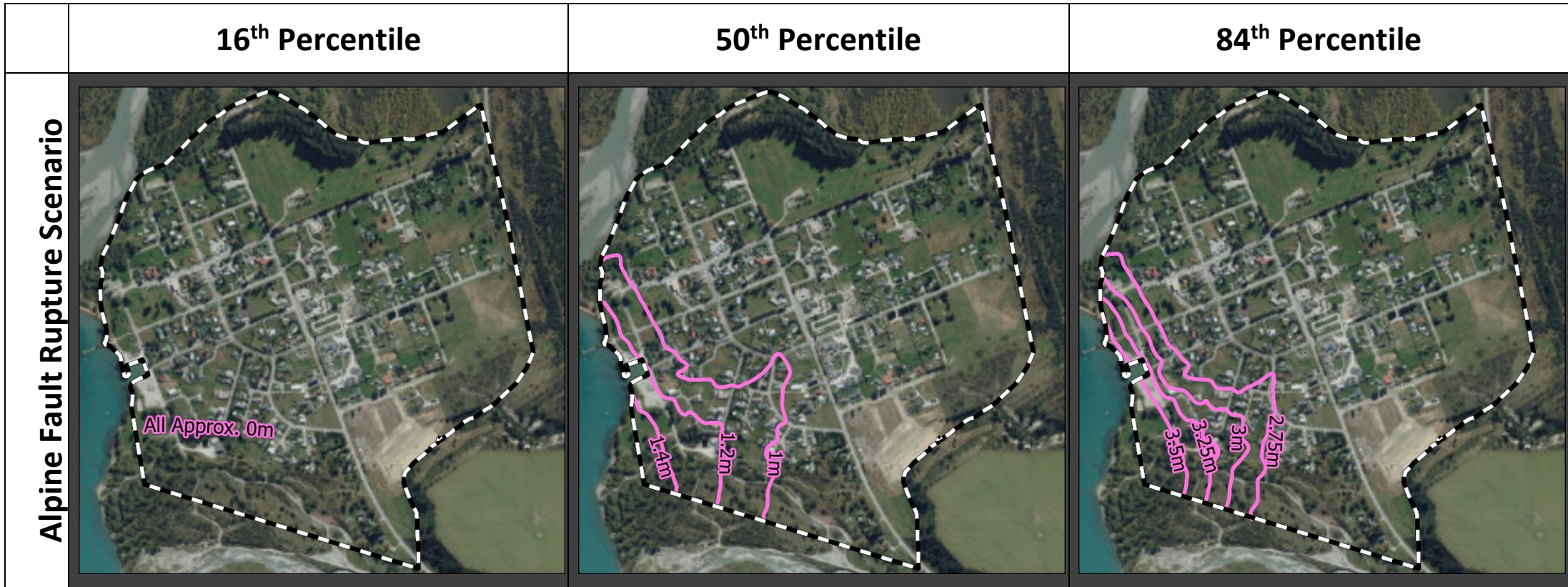*Table 13.2: Lateral Spreading for the Alpine Fault Rupture Scenario at different percentiles of shaking. The ground would be expected to move towards the lake by the annotated distance.*

16th Percentile	50th Percentile	84th Percentile

Alpine Fault Rupture Scenario

16th Percentile: All Approx. 0m

50th Percentile: 1.4m, 1.2m, 1m

84th Percentile: 3.5m, 3.25m, 3m, 2.75m

While lateral spreading movement can damage land (including causing significant vertical settlement), lateral stretch is what causes the most significant ground cracking and damage to infrastructure and buildings (refer to photos B4 to B9 in Appendix B). Lateral stretch is the differential spreading amount: i.e., if the front of a building moves 1m toward the lake and the back only moves 0.5m, the lateral stretch is 500mm over the length of the building. Based on the lateral spreading contours presented in Tables 13.1 and 13.2, the potential lateral stretch was estimated for a length scale of 25 metres (i.e., the length of a typical residential house) to identify the areas where the lateral spreading would have the most damaging effects. The various lateral spread damage zones are shown on Figure A1 in Appendix A.

Figure A1 in Appendix A shows that a significant western portion of Glenorchy would experience severe (>500mm) levels of lateral stretch, and an even larger portion would experience major (>200mm) lateral stretch for both the 500-year and Alpine Fault scenarios. These are the areas where the most severe lateral spreading damage are expected to occur. If the study were a greenfield that was being considered for development, then these major and severe lateral spread damage zones should be avoided based on the MBIE & MfE (2017) guidance.

However, the study area is an existing township and there is no guidance on what to do when major and severe lateral spreading damage zones are identified for existing developed areas. It is unlikely that the existing buildings will safely withstand the lateral spread damage. Without specific engineering design, residential buildings in these zones cannot be expected to safely withstand these levels of lateral stretch. For any new building work in these lateral spreading zones, Section 12.2.2 of the Canterbury Recovery Residential Guidance (MBIE, 2012) provides guidance for various levels of lateral stretch vulnerability. At major levels (between 200 and 500 mm), the most heavy duty robust foundation design option for residential buildings (i.e. the TC3 Type 2B system in the Canterbury Residential Guidance) could potentially be used subject to specific engineering assessment. This foundation system is approximately $50 to $100k over and above the cost of a residential house on conventional foundations. At severe levels (>500mm), more substantial engineering works are required, which are outside of the scope of the Canterbury Residential Guidance.

Severe liquefaction on flat ground away from lateral spreading areas can cause significant vertical subsidence through volumetric consolidation, as well as through loss of ejecta. Lateral spreading further compounds this vertical settlement effect. The vertical drop related to lateral spreading typically ranges from 3 to 15% of the horizontal predicted amount of lateral spread but can increase up to 50% when lateral spreading becomes larger. Refer to Figures B3, B5 and B9 in Appendix B for examples. Based on observations from the 2010–2011 Canterbury earthquakes and 2016 Kaikoura earthquake, when the lateral spreading becomes large, the crust has an increased tendency to break up into blocks and the performance becomes increasingly less predictable. Some blocks only drop vertically by a small amount whereas other blocks drop vertically by a larger amount. Sometimes larger vertical drops occur further away from the free face and the settlement of these blocks push and translate the blocks horizontally nearer the face. In the severe stretch zone (>500mm) the vertical drop due to lateral spreading for both the 500-year and Alpine Fault scenarios could be in the order of 0.5m to 1m in addition to the vertical settlement caused by liquefaction ejecta and volumetric consolidation. These levels of vertical settlement are likely to cause extensive damage to existing structures in the spreading zone.

Vertical subsidence poses a special concern in Glenorchy due to its effect on the flooding hazard. The large vertical subsidence for the properties nearer the lakefront could cause significant flood level issues following an earthquake event, since for the same flood level the inundation depth experienced by houses would be greater.

14   Final Map and Conclusion

Figure A1 in Appendix A shows the liquefaction vulnerability categorization developed according to the criteria in the MfE/MBIE Guidance and the framework shown in Figure 4.1. This has been developed based on the modelled liquefaction effects of vertical subsidence as well as lateral spread and stretch across multiple the earthquake scenarios, especially the 100-year and 500-year scenarios as well as the Alpine Fault Rupture scenario which is approximately equivalent to a 30-year return period event.

Liquefaction damage is considered possible across the entirety of Glenorchy, except along the slope up to Bible Terrace where the liquefaction vulnerability is deemed low. In the north and in west, liquefaction vulnerability is considered high, whereas towards the Bible Terrance this vulnerability is considered medium.

Overall, liquefaction poses a significant hazard to Glenorchy. The large cumulative thicknesses of liquefiable material (between 10 and 20m in most cases) together with a large 25m free face near the lake and relatively low-lying land together are likely to result in severe and widespread liquefaction damage in a medium to large earthquake. The hazard posed by the Alpine Fault is extremely high over the next 50 years and so the likelihood of a severe level of liquefaction damage, including severe damage from lateral spreading in the western side of Glenorchy occurring in the next 50 years is very high.

For comparison, in the worst affected areas of Christchurch where liquefaction and lateral spreading effects were observed, the cumulative thickness of liquefiable material was generally 10m or less; free face heights along the Avon River were 4m, and the groundwater is comparably shallow. In such areas, following the Canterbury earthquakes, the government deemed that land repair would be prolonged and uneconomic and so the land was 'red zoned'. The severity of damage to land, infrastructure and houses meant that solutions designed to deal with that level of damage, and prepare for comparable damage in the future, were not feasible at the time.

The vertical subsidence effects from liquefaction and lateral spreading are a special concern in Glenorchy owing to the lake flooding hazard. All areas experiencing significant vertical subsidence (in extreme cases predicted to be around 1m) would have an increased vulnerability to flooding. In the future, climate change is predicted to increase the frequency of flooding events in Glenorchy. The already high flooding risk would be further increased by any reduction in elevation from vertical subsidence following an earthquake.

15   References

Abrahamson, N., Silva, W., & Kamai, R. (2013). *Update of the AS08 Ground-Motion Prediction Equations Based on the NGA-West2 Data Set.* Berkeley: Pacific Earthquake Engineering Research Center, University of California, Berkeley.

Biasi, G. P., Langridge, R. M., Berryman, K. R., Clark, K. J., & Cochran, U. A. (2015). Maximum-Likelihood Recurrence Parameters and Conditional Probability of a Ground-Rupturing Earthquake on the Southern Alpine Fault, South Island, New Zealand. *Bulletin of the Seismological Society of America, 105*(1), 94-106. doi:10.1785/0120130259

Boore, D. M., Stewart, J. P., Seyhan, E., & Atkinson, G. M. (2014). NGA-West2 Equations for Predicting PGA, PGV, and 5% Damped PSA for Shallow Crustal Earthquakes. *Earthquake Spectra, 30*(3), 1057-1085. doi:10.1193/070113EQS184M

Boulanger, R., & Idriss, I. (2014). *CPT and SPT Based Liquefaction Triggering Procedures.* Center for Geotechnical Modeling, University of California.

Bradley, B., Bae, S., Polak, V., Lee, R., Thomson, E., & Tarbali, K. (2017). Ground motion simulations of great earthquakes on the Alpine Fault: effect of hypocentre location and comparison with empirical modelling. *New Zealand Journal of Geology and Geophysics*, 188-198. doi:10.1080/00288306.2017.1297313

Bray, J., & Macedo, J. (2019). Procedure for Estimating Shear-Induced Seismic Slope Displacement for Shallow Crustal Earthquakes. *Journal of Geotechnical and Geoenvironmental Engineering*.

Campbell, K. W., & Bozorgnia, Y. (2014). NGA-West2 Ground Motion Model for the Average Horizontal Components of PGA, PGV, and 5% Damped Linear Acceleration Response Spectra. *Earthquake Spectra, 30*(3), 1087-1115. doi:10.1193/062913EQS175M

e3 Scientific Ltd. (2018). *Environmental effects of On-site Sewage Management in Glenorchy, Stage 2: Investigations.* Arrowtown: e3 Scientific Limited.

Gillins, D., & Bartlett, S. (2014). Multilinear Regression Equations for Predicting Lateral Spread Displacement from Soil Type and Cone Penetration Test Data. *Journal of Geotechnical and Geoenvironmental Engineering*.

Howarth, J., Barth, N., Fitzsimons, S., Richards-Dinger, K., Clark, K., Biasi, G., . . . Sutherland , R. (2021). Spatiotemporal clustering of great earthquakes on a transform fault controlled by geometry. *Nature Geoscience*, 314-320. doi:10.1038/s41561-021-00721-4

MBIE & MfE. (2017). *Planning and Engineering Guidance for Potentially Liquefaction-prone Land.* Wellington: New Zealand Ministry of Business, Innovation and Employment, Building System Performance Branch.

MBIE. (2012). *Repairing and rebuilding houses affected by the Canterbury earthquakes* (3rd ed.). Wellington: Ministry of Business Innovation and Employment.

MBIE. (2022, January 20). *NZGD Homepage*. Retrieved from New Zealand Geotechnical Database: https://www.nzgd.org.nz/

NZGS & MBIE. (2021a). *Earthquake geotechnical engineering practice, Module 1: Overview of the Guidelines.* Wellington: New Zealand Geotechnical Society and Ministry of Business, Innovation and Employment.

NZGS & MBIE. (2021b). *Earthquake geotechnical engineering practice, Module 3: Identification, assessment and mitigation of liquefaction hazards.* Wellington: New Zealand Geotechnical Society and Ministry of Business, Innovation and Employment.

NZTA. (2013). *Bridge manual* (3rd ed.). Wellington: New Zealand Transport Agency.

Stirling, M., McVerry, G., Gerstenberger, M., Litchfield, N., Van Dissen, R., Berryman, K., . . . Jacobs, K. (2012, August). National Seismic Hazard Model for New Zealand: 2010 Update. *Bulletin of the Seismological Society of America, 102*(4), 1517-1519. doi:10.1785/0120110170

Youd, T., Hansen, C., & Bartlett, S. (2002). Revised Multilinear Regression Equations for Prediction of Lateral Spread Displacement. *Journal of Geotechnical and Geoenvironmental Engineering*.

Zhang, G., Robertson, P., & Brachman, R. (2004). Estimating Liquefaction-Induced Lateral Displacements Using the Standard Penetration Test or Cone Penetration Test. *Journal of Geotechnical and Geoenvironmental Engineering*.

16   Applicability

This report has been prepared for the exclusive use of our client Otago Regional Council, with respect to the particular brief given to us and it may not be relied upon in other contexts or for any other purpose, or by any person other than our client, without our prior written agreement.

The susceptibility analyses carried out represent probabilistic analyses of empirical liquefaction databases under various earthquakes. Earthquakes are unique and impose different levels of shaking in different directions on different sites. The results of the liquefaction susceptibility analyses, and the estimates of consequences presented within this document are based on regional seismic demand and published analysis methods, but it is important to understand that the actual performance may vary from that calculated.

This assessment has been made at a broad scale across Glenorchy and is intended to describe the typical range of liquefaction vulnerability across neighbourhood-sized areas. It is not intended to precisely describe liquefaction vulnerability at individual property scale. This information is general in nature, and more detailed site-specific liquefaction assessment may be required for some purposes (e.g., for design of building foundations).

Tonkin & Taylor Ltd

Report prepared by: Authorised for Tonkin & Taylor Ltd by:

....

Nathan McDougall   Sjoerd van Ballegooy
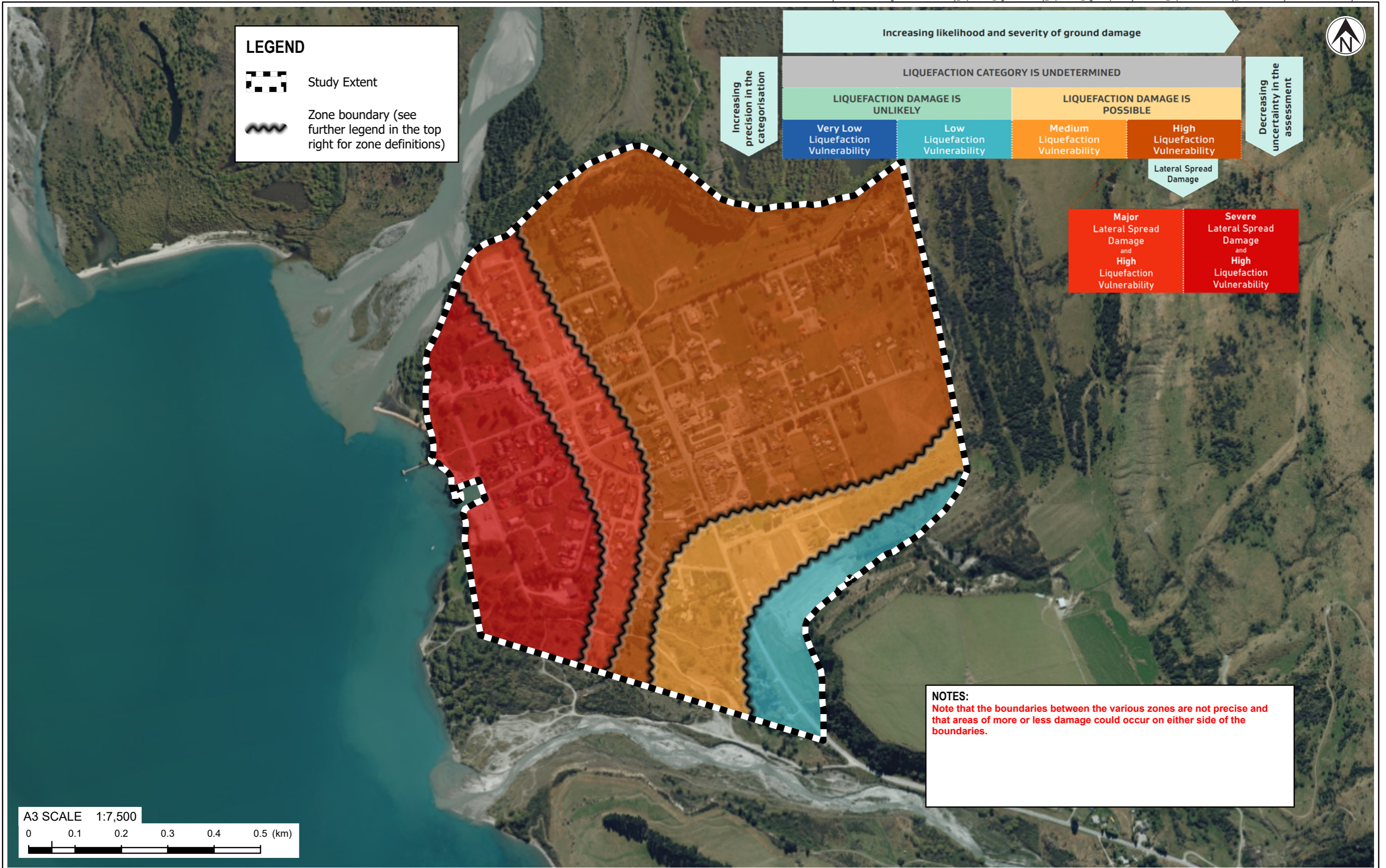
Engineer   Project Director & Technical Director

Appendix A: Map of liquefaction and lateral spreading damage potential zones

LEGEND

Study Extent

Zone boundary (see further legend in the top right for zone definitions)

Increasing likelihood and severity of ground damage

Increasing precision in the categorisation

Decreasing uncertainty in the assessment

LIQUEFACTION CATEGORY IS UNDETERMINED

LIQUEFACTION DAMAGE IS UNLIKELY

LIQUEFACTION DAMAGE IS POSSIBLE

Very Low Liquefaction Vulnerability	Low Liquefaction Vulnerability	Medium Liquefaction Vulnerability	High Liquefaction Vulnerability

Lateral Spread Damage

Major Lateral Spread Damage and High Liquefaction Vulnerability	Severe Lateral Spread Damage and High Liquefaction Vulnerability

NOTES:
Note that the boundaries between the various zones are not precise and that areas of more or less damage could occur on either side of the boundaries.

A3 SCALE   1:7,500

0   0.1   0.2   0.3   0.4   0.5 (km)

PROJECT No.	1017916.2000		CLIENT	**OTAGO REGIONAL COUNCIL**
DESIGNED	NAMC	MAY.22	PROJECT	**GLENORCHY LIQUEFACTION STUDY**
DRAWN	NAMC	MAY.22		
CHECKED			TITLE	LIQUEFACTION VULNERABILITY (MFE/MBIE CLASSIFICATION) AND LATERAL SPREADING DAMAGE ZONES

1	Second version		NAMC	YYYY	16/05/22
REV	DESCRIPTION		GIS	CHK	DATE

LOCATION PLAN   APPROVED   DATE

SCALE (A3)	1:7,500	FIG No.	FIGURE A1	REV	1

Tonkin+Taylor

Exceptional thinking together   www.tonkintaylor.co.nz

Appendix B: Maps and photos showing examples of the liquefaction and lateral spreading that was observed following the 2010-2011 Christchurch earthquakes and 2016 Kaikoura earthquakes
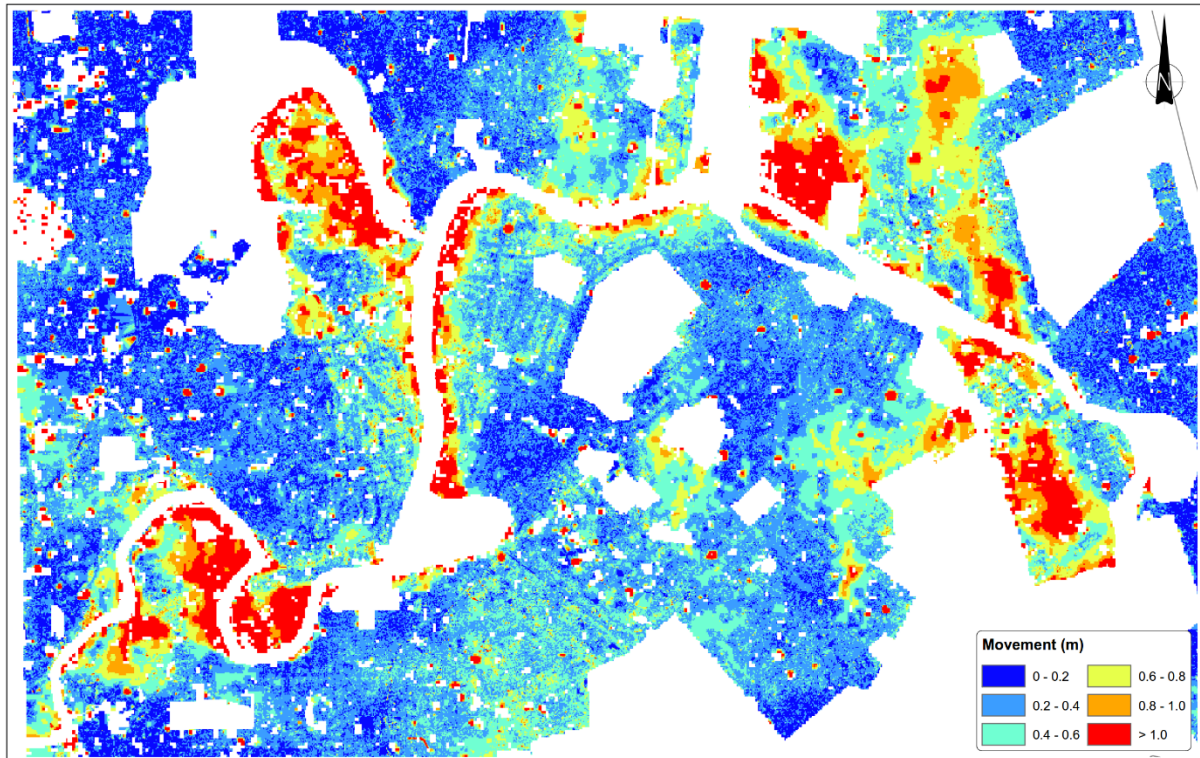
Figure B1 - Map showing the extent of lateral spreading in the eastern suburbs of Christchurch. The maximum lateral spread was approximately 3m.
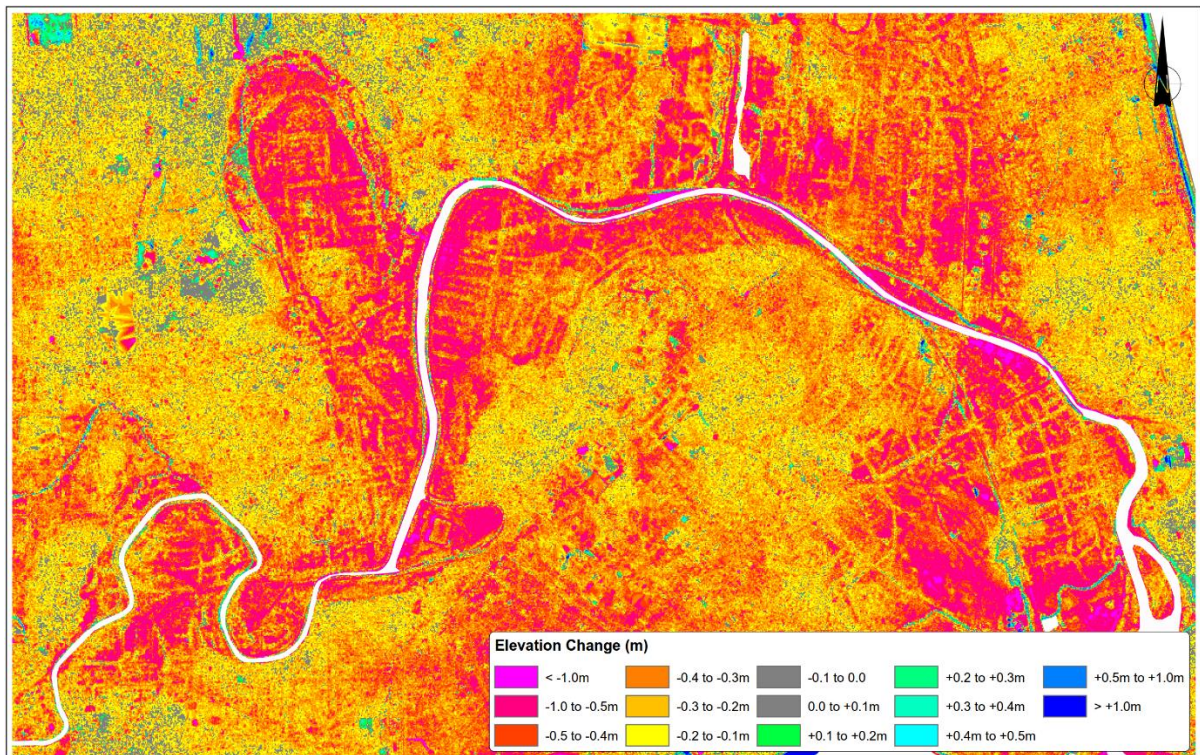

Figure B2 - Map showing the ground surface subsidence in the eastern suburbs of Christchurch due to liquefaction and lateral spreading. Visual comparison with Figure B1 shows that the areas where lateral spreading occurred have a significantly higher subsidence. This demonstrates that lateral spreading significantly increases subsidence.

Figure B3 – Photo showing the lateral spreading that occurred in Blenheim at a vineyard along the Wairau River following the 2016 Kaikoura earthquake. The lateral spreading horizontal movement was approximately 3m and the vertical drop was approximately 1m (approx. 33% of the horizontal movement).

Figure B4 - Photo showing lateral spreading effects at Courtenay Drive, Kaiapoi following the 2010 Darfield earthquake. The ground crack filled up with liquefied sand and resulted in a significant evacuation hazard following the event. The lateral spreading at this site was approximately 2m.

Figure B5 - Photo showing lateral spreading effects at Courtenay Drive, Kaiapoi following the 2010 Darfield earthquake. The lateral spreading caused approximately 1m of horizontal stretch and also a 300mm vertical offset. The total lateral spreading at this site was approximately 2m.

Figure B6 - Photo showing lateral spreading effects at Courtenay Drive, Kaiapoi following the 2010 Darfield earthquake. The total lateral spreading at this site was approximately 2m.

Figure B7 - Photo showing lateral spreading effects at Courtenay Drive, Kaiapoi following the 2010 Darfield earthquake. The total lateral spreading at this site was approximately 2m. If the lateral spreading at the site had been higher, this building would likely have collapsed.

Figure B8 - Photo showing lateral spreading at Charles Steet, Kaiapoi following the 2010 Darfield earthquake. The total lateral spreading at this site was approximately 1.5m. Vertical offsets in the order of 300mm can also be seen in the photo (approx. 20% of the horizontal movement).

Figure B9 - Photo showing lateral spreading at Fitzgerald Ave, Christchurch following the 2011 Christchurch earthquake. The total lateral spreading at this site was approximately 2m. Vertical offsets in the order of 500mm (approx. 50% of the horizontal movement).

Figure B10 - Photo showing liquefaction in Christchurch following the 2011 Christchurch earthquake. Approximately 400 to 500mm of liquefaction ejecta inundated the roads.

Figure B11 - Photo showing liquefaction in Christchurch following the 2011 Christchurch earthquake. Approximately 200mm to 300mm of liquefaction ejecta inundated the roads.

Figure B12 - Photo showing liquefaction in Christchurch following the 2011 Christchurch earthquake. There were significant roadway stability issues causing significant evacuation hazards.